1986ApJ...307....1S

THE ASTROPHYSICAL JOURNAL, 307:1–19, 1986 August 1
© 1986. The American Astronomical Society. All rights reserved. Printed in U.S.A.

THE REDSHIFT-DISTANCE RELATION. IX. PERTURBATION OF THE VERY NEARBY VELOCITY FIELD BY THE MASS OF THE LOCAL GROUP

ALLAN SANDAGE
Mount Wilson and Las Campanas Observatories of the Carnegie Institution of Washington
Received 1985 August 26; accepted 1986 January 21

ABSTRACT

The deceleration of the very local cosmological velocity field that is expected as a result of the mass of the Local Group is calculated for assumed Local Group masses of 0, 5×10^{11}, 2×10^{12}, 5×10^{12}, and 2×10^{13} $M_\odot$ in a $\Omega_0 = 0$ space. The predicted decelerations are illustrated in the three equivalent representations of (1) deviations from linearity of the local velocity-distance relation, (2) corrections to the centroidal velocities to account for the deceleration, and (3) the variation of the v/r Hubble ratio with distance.

The available velocities and distances of 20 nearby galaxies which have modern primary data are compared with the predictions using the standard solar motion corrections to the velocity data. A deceleration may have been detected, giving a best-fit mass of 4×10^{11} $M_\odot$ for the Local Group. The *upper limit* permitted by the data is $M_{LG} \sim 3 \times 10^{12}$ $M_\odot$, giving an upper limit to the mass-to-light ratio of ≈ 25. The best-fit value gives $M/L = 3$, providing no evidence for a supermassive halo, either for our Galaxy or for M31. With $M_{LG} = 4 \times 10^{11}$ $M_\odot$, the distance to an idealized zero-velocity surface for the Local Group is 0.8 Mpc.

The result is compared with that obtained from the classical Kahn-Woltjer timing calculation using the motion of M31 and the Galaxy alone. To do that requires a new solution for the solar motion relative to the centroid of the Local Group. If the model of the problem would be precise, the Galaxy must be moving directly toward M31. With this constraint, an exploration of the parameter space of the value of the Galactic rotation at the solar circle, the solar motion relative to the centroid, and the Galactic motion toward M31 is made. The resulting optimum solar motion of 295 km s^{-1} toward $l = 97\overset{\circ}{.}2$, $b = -5\overset{\circ}{.}6$ is adopted. A Kahn-Woltjer calculation using this new solar motion still gives the traditional mass discrepancy of a factor of 7 above the optimum mass from the deceleration method for the combined M31 plus galaxy mass. If the discrepancy is real, the velocity of approach of M31 and the Galaxy must have a random velocity component in addition to that from the ideal model.

The deceleration calculations for the massless Local Group satellite galaxies are repeated for a $\Omega_0 = 1$ space with the result that $M_{LG} \sim 8 \times 10^{11}$ $M_\odot$, but, because there is no other observational support for a $\Omega_0 = 1$ universe, we reject the result as being unrealistic.

The calculated deceleration due to the Local Group is so small that it cannot explain any supposed variation of the Hubble constant with distance beyond ~ 2 Mpc. If $M_{LG} = 5 \times 10^{11}$ $M_\odot$, the Hubble v/r ratio reaches 83% of its far-field value at a distance of 2 Mpc and 98% at 4 Mpc for the $\Omega_0 = 0$ case, neglecting other decelerating sources such as the Virgo cluster.

The data give an upper limit of $\sigma(v) = 60$ km s^{-1} for the mean random motion about the predicted velocity-distance relation for the local galaxies. The true random motion is, of course, smaller, considering the uncertainties in the adopted distances, a fact which itself requires a low Local Group mass of $\sim 4 \times 10^{11}$ $M_\odot$ *if* the group is virialized.

Subject headings: cosmology — galaxies: Local Group — galaxies: redshifts — galaxies: structure

I. INTRODUCTION

The velocity-distance relation is linear to high accuracy when mapped using the brightest several E galaxies in groups and clusters (Sandage and Hardy 1973, Paper VII). Any systematic deviation from linearity that may be present is near the limit of detection using the residuals of the redshift-magnitude relation of the E galaxy sample (Sandage and Tammann 1975; Sandage 1975, Paper VIII).

On the other hand, alternate methods used by other workers in the past to determine distances had suggested large systematic deviations from linearity (see de Vaucouleurs 1958, 1964, 1972). These results have been interpreted either as a large-scale phenomenon caused by a globally hierarchical universe in which the mean density decreases outward (Wertz 1971; Haggerty annd Wertz 1971), or by a very large local deviation caused by the Virgo complex (de Vaucouleurs 1958, 1964, 1972) that must then, perforce, be massive.

Predictions using the particular hierarchical model of Wertz and of Haggerty and Wertz were tested (Sandage, Tammann, and Hardy 1972) using available E galaxy observations, but no evidence was found from the velocity residuals for a deviation from homogeneity of the universe *in the large*. The Wertz "hierarchical decay constant" [defined through $\langle \rho(r) \rangle \sim r^{-\theta}$] is $\theta \approx 0$ to within the observational accuracy. The appeal, then, to a hierarchical universe to justify an apparent change of the expansion rate with distance becomes ad hoc.

Another interpretation is that the apparent change of the Hubble rate with distance is not real, but rather is caused either by selection effects in any particular data set (van Albada 1962, in one of the first statements of an observational bias for

© American Astronomical Society • Provided by the NASA Astrophysics Data System

1986ApJ...307....1S

this particular problem) or by more basic deficiencies in the particular method used to obtain distances (de Vaucouleurs 1975, pp. 261–265; Giraud 1986*a*, *b*, *c*, in his critique of the Tully-Fisher method as currently applied).

Over the distance range that is more restricted than that for a large-scale systematic global hierarchical effect, a perturbation of the velocity field *is* expected at some level due to the Virgo complex. This effect has been searched for extensively in recent years, following the repeated results of de Vaucouleurs. Peebles (1976) tested the idealized Virgocentric perturbation model of Silk (1974) using the field galaxy data available at that time (Sandage and Tammann 1975) and found support for a velocity variation due to Virgo at the position of the Local Group of ~ 250 km s^{-1}. Following the initial work of de Vaucouleurs and Peebles, this infall signal now seems to have been definitely detected at a level of $v_{vc} \approx 220$ km s^{-1}. There is agreement between all observers of its value to within about a factor of 2 (see Tammann and Sandage 1985 for a review of the literature to the end of 1984).

Finally, for the very nearby galaxies the Local Group must similarly perturb the velocity field over distances much smaller than the effect caused by the overdensity of the Virgo complex. The expected distance range within which this effect occurs is $0 < D \lesssim 5$ Mpc, based on reasonable values of the mass ratio of the Local Group to the Virgo complex (see Einasto and Lynden-Bell 1982).

An observational detection of the velocity perturbation by the Local Group is of considerable interest for a number of reasons. Comparison of the observations with the theory could set limits on (1) the mass of the Local Group determined from the observed deceleration of the satellite galaxies that are both inside and outside the present position of the zero-velocity surface of the Local Group, (2) the mass of the Local Group from the position of the zero-velocity surface itself (Lynden-Bell 1981), (3) any zero-point offset in the velocity-distance relation at very small distances that is predicted by most hierarchical density models (Wertz 1971, Fig. 2; Haggerty and Wertz 1971, Fig. 1), (4) the expected change of the apparent Hubble constant with distance from the Local Group depending on the Local Group mass M_{LG} and hence on whether the effects said to be observed, viz. that $H = H(r)$ locally (i.e., over the first ~ 10 Mpc from us) can be due to Local Group deceleration, or due only to observational bias in the data set, and finally (5) the mean random motion about an ideal Hubble flow exhibited by the very local galaxies.

Concerning point (5), the question of whether a random motion indeed exists is fundamental to much of the large body of literature now available on the genesis and mass of the Local Group (see Lynden-Bell 1982; Lynden-Bell, Cannon, and Godwin 1983, and earlier references therein), following the fundamental paper on the timing argument for the turnaround of M31 (because it is approaching our Galaxy) first made by Kahn and Woltjer (1959). If random motions exist of an unknown origin (presumably due to local torques) not connected with the zero angular momentum model of the ideal big-bang dynamics, a scatter in the data will exist, causing uncertainties in the true motion "generated by the gravity field of the Local Group heavyweights" (Lynden-Bell 1983, p. 362). Calculations based on the ideal big-bang dynamics will then be spoiled for any given galaxy to a degree that depends on the size of the random motions. In this case, averages of the velocity and distance data of nearby galaxies might be expected to overcome the random motion problem, retaining the basic philosophy of the big-bang dynamical calculation. The present paper is written in this spirit—that the deceleration of the velocity field due to the Local Group might be measured by considering the aggregate of data now available on velocities and distances of galaxies closer than ~ 10 Mpc, rather than relying solely on the infall of, say, only M31 toward the Galaxy. Lynden-Bell's (1981) method of using the position of the zero velocity surface, generalized to the aggregate deceleration field itself, can then be applied to the total data rather than to individual objects.

The purpose of the present paper is to use what new data are now available on distances less than ~ 10 Mpc, comparing them with the dynamical models to discuss the five points previously mentioned. The paper is presented as a series of successive approximations, starting from the simplest dynamical case and progressively adding more detail to the kinematical and dynamical model.

Calculation of the expected decelerations due to the mass of the Local Group is made in the next section for a $\Omega_0 = 0$ space into which test particles are injected from the Local Group centroid with a continuum of energies. Because the space is otherwise empty except for a centralized Local Group mass, this deceleration is described by the two-body problem with zero angular momentum and a constant central mass.

The predictions are compared with the available observational data on velocities and distances of very nearby galaxies in § III using the standard solar motion correction which reduces all observed heliocentric velocities to the centroid of the Local Group. There, a first estimate of the mass of the Local Group is obtained.

A refinement of the solar motion correction is made in § IV where we take the dynamical model seriously be requiring (1) M31 and the center of our Galaxy to be moving precisely toward each other and (2) the center of mass (the centroid) of the Local Group to be on the line joining them. This constrains the value of the velocity of the center of our Galaxy for any given solar motion relative to the centroid. With this constraint, we explore the parameter space composed of the value of the solar motion relative to the Local Group, the motion of the Galactic center toward the centroid, and the velocity of approach of M31 and the Galaxy. In this way, we arrive at a new value of the solar motion. This is applied to the basic heliocentric velocity data to obtain a second approximation to the corrected observational data for the test galaxies (assumed to be massless), excluding M31 and our Galaxy to which different dynamics must be applied because these two are not massless but constitute the total mass of the Local Group.

These second-approximation data are compared again in § V with the model predictions, still for the $\Omega_0 = 0$ space, and the optimum values of the Local Group mass and mass-to-light ratio are obtained again. The effect on M_{LG} of changing the time scale (i.e., by adopting different Hubble constants) is also discussed in this section.

The mass obtained in § V is compared in § VI with the mass of M31 plus the Galaxy calculated from a detailed application of the original Kahn-Woltjer timing argument.

In § VII the expected deceleration is recalculated for an outside space that has matter uniformly distributed at the critical closure density of $\langle \rho \rangle = 3H_0^2/8\pi G$, i.e., for $\Omega_0 = 1$, and the resulting models are again compared with the second-approximation observational data to obtain M_{LG} once more.

© American Astronomical Society • Provided by the NASA Astrophysics Data System

1986ApJ...307....1S

Finally, in § VIII the mass-to-light ratio that follows from the present results is compared with other data in the recent literature.

II. CALCULATED DECELERATION FOR LOCAL GALAXIES IN A $\Omega_0 = 0$ SPACE

A linear velocity field at all times, everywhere, is naturally generated kinematically if projectiles were to be released from an origin with different initial velocities and injected into a force-free field. Being force-free, there is no deceleration—the initial velocity of each particle is its velocity forever; the distance covered at any time after release varies directly with the velocity.

This, of course, is not a picture of the expansion of the universe. If it were, we could not explain the homogeneous distribution of galaxies in the large (i.e., approximately equal numbers of galaxies per unit proper volume) without postulating an unrealistic initial velocity distribution for the emitted particles.

The big-bang model is not where galaxies expand into a space already there, but rather, where space itself expands, carrying the galaxies with it, thereby insuring large-scale homogeneity as long as the geometry of the spatial manifold itself is homogeneous and isotropic. It is the change of the scale factor $R(t)$ of this homogeneous manifold that is the solution of the Friedmann equation of classical cosmology, where, given the force field of the universe itself, the deceleration $\ddot{R}$ can be calculated.

Nevertheless, the formalism of the local dynamics can be imitated by a strictly Newtonian calculation. The problem can be modeled by considering massless test particles emitted simultaneously with different velocities (energies) from an origin (in this case, the Local Group). The velocities and distances of each particle can then be calculated at any given time after the release. The approximation calculated in this section is for test particles thrown into free space devoid of any matter except that of the Local Group treated as a point mass. Hence $\Omega_0 = 0$ in the large for this model.

a) *Solution of the Equation of Motion*

We need the equation of the path $r(t)$ of any given test particle emitted radially from the centroid of the Local Group at time $t = 0$.

The equation of motion is

$$\ddot{r} = -\frac{GM}{r^2}, \tag{1}$$

where M is the total mass of the Local Group.

Integrating once gives the energy equation

$$\dot{r}^2 - \frac{2GM}{r} = 2E, \tag{2}$$

which is identical to the familiar Friedmann cosmological equation for the manifold scale factor $R(t)$:

$$\frac{\dot{R}^2}{R^2} + \frac{2\ddot{R}}{R} + \frac{8\pi G p}{c^2} = \frac{-kc^2}{R^2} + \Lambda c^2 \tag{3}$$

(see Robertson 1933, eq. [3.2]; McCrea 1953, eq. [7.8]; Sandage 1961*a*, eq. [2]; McVittie 1965, eq. [8.210]) when the pressure, p, and the cosmological constant, Λ, are put to zero, and if r is identified with R, equation (1) of the motion is used to eliminate $\ddot{R}$ from equation (3), and the energy in equation (2) is identified as $-\frac{1}{2}kc^2$.

It is well known (see Sandage 1961*b*, eqs. [3]–[6]; Lynden-Bell 1981, eq. [2]) that the solution to equations (2) and (3) is

$$r = \frac{GM}{-2E}(1 - \cos\theta), \tag{4}$$

$$t = \frac{GM}{(-2E)^{3/2}}(\theta - \sin\theta), \tag{5}$$

for negative energies, and

$$r = \frac{GM}{2E}(\cosh\theta - 1), \tag{6}$$

$$t = \frac{GM}{(2E)^{3/2}}(\sinh\theta - \theta), \tag{7}$$

for positive energies. These are the parametric equations for a cycloid when the system is bound, and of a hypercycloid when $r(t)$ increases without limit.[1]

We require the velocity-distance relation for the system of particles at any designated time, T, given that the particles have different initial velocities determined by the values of E that are chosen to produce the family.

Consider first the system of particles that have not been given high enough velocities to escape the pull of the Local Group. The energy of such particles is negative. They will proceed outward for a time, halt, and eventually fall back toward the origin. If we assign a continuum of energies E to them, we produce a continuum of $r(t)$ curves that can be calculated from equations (4) and (5). For any given energy E, at any given time t, the development angle (which represents the degree of unfolding of the cycloid) can be calculated from equation (5), which, when applied in equation (4), gives the distance of the particle at the particular time t, leading directly to the velocity-distance relation at that time.

The velocity of the particle of energy E at this particular time follows from equation (4) and (5) as

$$v = \frac{dr}{dt} = \frac{dr}{d\theta}\frac{d\theta}{dt} = \frac{GM}{\sqrt{-2E}}\frac{\sin\theta}{r}, \tag{8}$$

which, together with equation (4), can be made to define the required set of r, v values as E (and hence θ) is varied.

An analogous calculation can be made for the positive energy case, where the equivalent of equation (8) is

$$v = \frac{GM}{\sqrt{2E}}\frac{\sinh\theta}{r}, \tag{9}$$

which, together with equation (6) using θ which is calculated from equation (7) assuming a value for the time t and assuming different E values, produces a single r, v curve as E is varied (at constant time t) for a given value of M_{LG}. A family of such r, v curves for given values of E can be produced (at a fixed time t) as M_{LG} is varied. In this way, the deceleration caused by the Local Group can be calculated for any assumed mass.

[1] Many of the relations in cosmology that contain only the observables of luminosity, redshift, angular diameter, and number per magnitude interval can be derived most easily using this development angle formalism. Some of these are given elsewhere (Sandage 1961*b*, 1962), where the constants a and c in those references are $a = GM/(-2E)$, $c = (-2E)^{1/2}$, and $c/a = (-2E)^{3/2}/GM$ for the present problem.

© American Astronomical Society • Provided by the NASA Astrophysics Data System

1986ApJ...307....1S

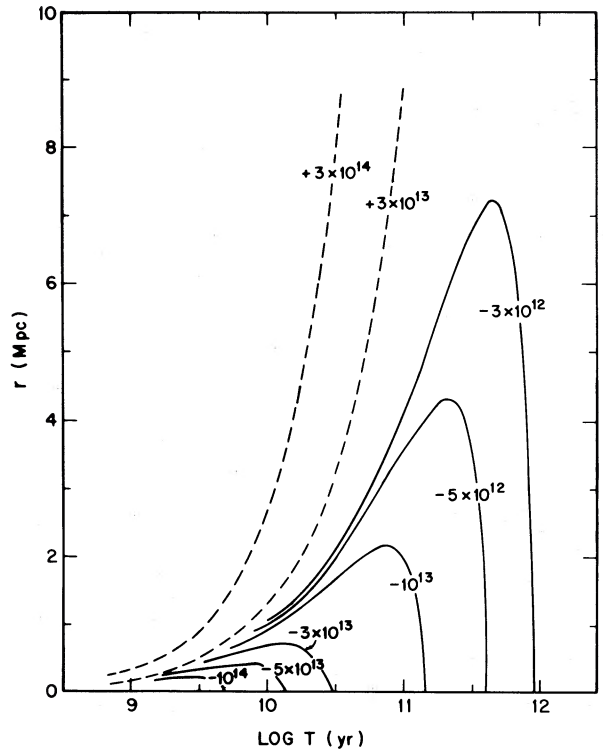

FIG. 1.—Solution of eq. (2) for the motion of particles with zero angular momentum in an attractive inverse square force field as the total energy is varied. Solid curves are the cases with negative energy (cycloids); two dashed curves are cases with positive energy (hypercycloids) with no turnaround. These particular solutions are from eqs. (4)–(7) assuming a Local Group mass of $5 \times 10^{11}\ M_\odot$.

The procedure is illustrated in Figure 1 which gives the results for a family of $r(t)$ curves calculated for an assumed mass of the Local Group of $5 \times 10^{11}\ M_\odot$ for a series of energies that vary between -10^{14} and $+3 \times 10^{14}$ cgs units. Six negative energy values are shown. The curves are cycloids, each reaching a maximum distance r(max) where the velocity is zero; the test particle then falls back toward the origin.

Two positive energy hypercycloid paths are shown as dashed curves. Here the particles have initial velocities higher than the escape velocity, and r increases without bound forever. (The curves do not look like cycloids and hypercycloids because of the compression of the abscissa at large times due to the logarithmic time plot.)

The calculations for Figure 1 were made from equations (4)–(7), converted to distances in megaparsecs and times in years via

$$r = \frac{2.161 \times 10^{13}}{(-2E)} (1 - \cos\theta)\ \text{Mpc}\ , \qquad (10)$$

$$t = \frac{2.123 \times 10^{30}}{(-2E)^{3/2}} (\theta - \sin\theta)\ \text{yr}\ , \qquad (11)$$

for the negative energy family, with analogous hyperbolic expressions following equations (6) and (7) using the same numerical factors for positive energy.

b) *The Velocity-Distance Relation Perturbed by the Local Group*

The velocity-distance relation exhibited by the continuum of curves, of which only eight are shown in Figure 1, changes with time. If we wish to calculate a particular v, r relation at a particular time t, we must fix t in equation (11), which then fixes the value of the development angle θ for any energy value. This angle, now at given t and E, gives the distance via equation (10). The velocity from equation (8) produces one r, v pair. The calculation is continued for other E values to produce a series of r, v pairs, which is, of course, the required velocity-distance relation. A family of such r, v curves can be calculated in the same way by varying $M_{\rm LG}$.

An intuitive appreciation of the calculation can be obtained by considering a vertical line in Figure 1 at some particular time t, such as $\log t = 10.30$ after the beginning. The tightly bound particles with the large negative energies of -10^{14} to -5×10^{13} cgs have turned around and have reached the origin again. They will have passed through the origin and will have begun a second swing on the other side of the origin when $\theta > 2\pi$, not shown in Figure 1.

In Figure 1, the particle with $E = -3 \times 10^{13}$ cgs has reached its maximum extent at $\theta = \pi$, is retreating again toward the origin $r = 0$, and hence has a negative velocity (i.e., $\theta > \pi$ at $\log t = 10.3$; cf. eq. [8]). This is evident graphically from Figure 1 because the sign of the tangent dr/dt to the curve at $\log t = 10.3$ is negative. The remaining five curves have positive dr/dt slopes at this particular time.

The time at which we draw the vertical line in Figure 1 is not arbitrary if we wish a particular far-field (global) value of the Hubble constant. Clearly, as the vertical line in Figure 1 is moved toward the right, the distance at a given velocity increases, and the apparent Hubble ratio decreases as t increases. We have adjusted the calculations to fit the observed mean velocity-distance ratio at large r as required by the adopted data in § III. For the calculated v, r relation, t is then fixed in equations (5) and (7), giving, from these equations, $\theta = f(E)$ which solves the problem by substituting this correspondence into equations (4) and (8), or equations (6) and (9), for any assumed value of $M_{\rm LG}$.

The result is shown in Figure 2 for five values of the Local Group mass. The top curve that passes through the origin is for zero mass. There is no deceleration. The velocity of any particle remains constant at all times.

The remaining four curves are the predicted velocity-distance relations for masses of 5×10^{11}, 2×10^{12}, 5×10^{12}, and $2 \times 10^{13}\ M_\odot$ for the Local Group, normalized to the far-field value of $v/r = 55\ \text{km s}^{-1}\ \text{Mpc}^{-1}$.

The parametric equations from which these curves have been calculated in this manner are

$$(-2E)^{3/2} = 2.332 \times 10^{8} M_{\rm LG} (\theta - \sin\theta)\ \text{cgs}\ , \qquad (12)$$

$$r = \frac{43.23 M_{\rm LG}}{(-2E)} (1 - \cos\theta)\ \text{Mpc}\ , \qquad (13)$$

$$v = \frac{4.323 \times 10^{-4}}{\sqrt{-2E}} M_{\rm LG} \frac{\sin\theta}{r}\ \text{km s}^{-1}\ , \qquad (14)$$

for the negative energy case, with identical numerical values for the positive energy case, but with the hyperbolic forms of equations (6), (7), and (9).

c) *Correction of Observed Velocities for Deceleration and the Change of the Hubble Ratio with Distance*

The deceleration of nearby galaxies shown in Figure 2, caused by the Local Group, is given in the more direct representation of Figure 3 as the correction to observed velocities

© American Astronomical Society • Provided by the NASA Astrophysics Data System

1986ApJ...307....1S

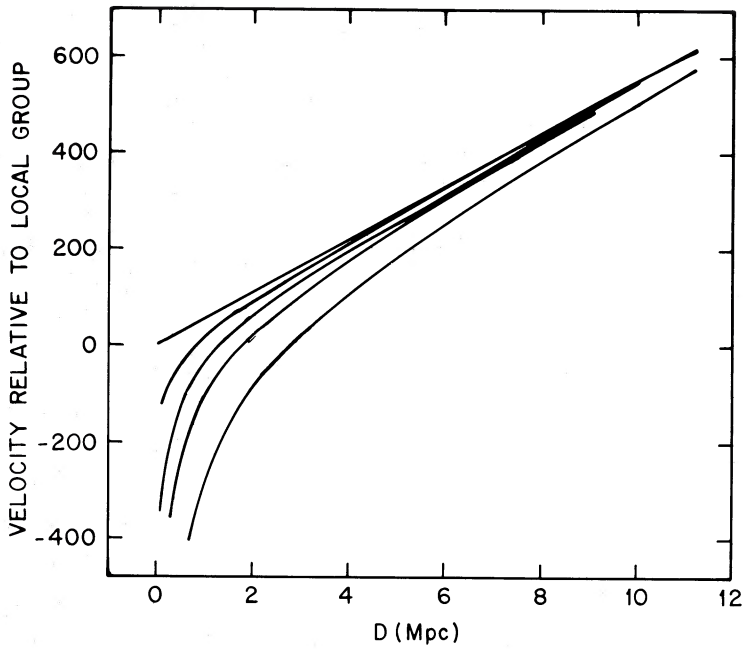

FIG. 2.—Predicted velocity-distance relations for Local Group masses of 0, 5×10^{11}, 2×10^{12}, 5×10^{12}, and 2×10^{13} $M_{\odot}$, respectively. Intersection of each curve with $v = 0$ locates the distance r_0 of the zero velocity surface at the present epoch ($H_0 = 55$ assumed), given analytically by eq. (18).

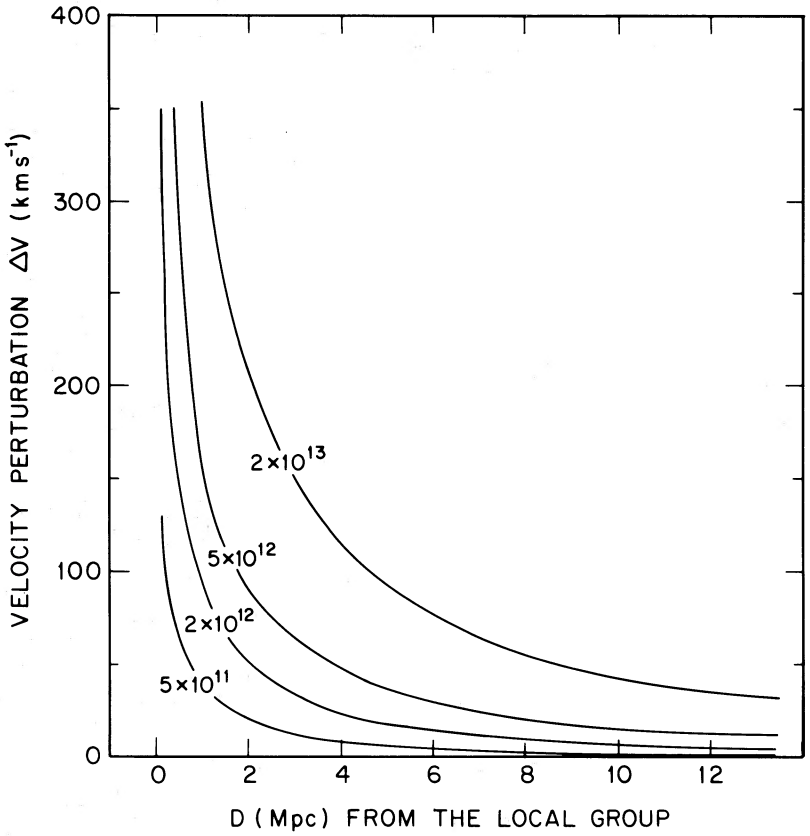

FIG. 3.—Correction to be applied to observed velocities to correct for deceleration of the Local Group for four assumed Local Group masses. The information is the same as in Fig. 2, but in a different representation.

© American Astronomical Society • Provided by the NASA Astrophysics Data System

1986ApJ...307....1S

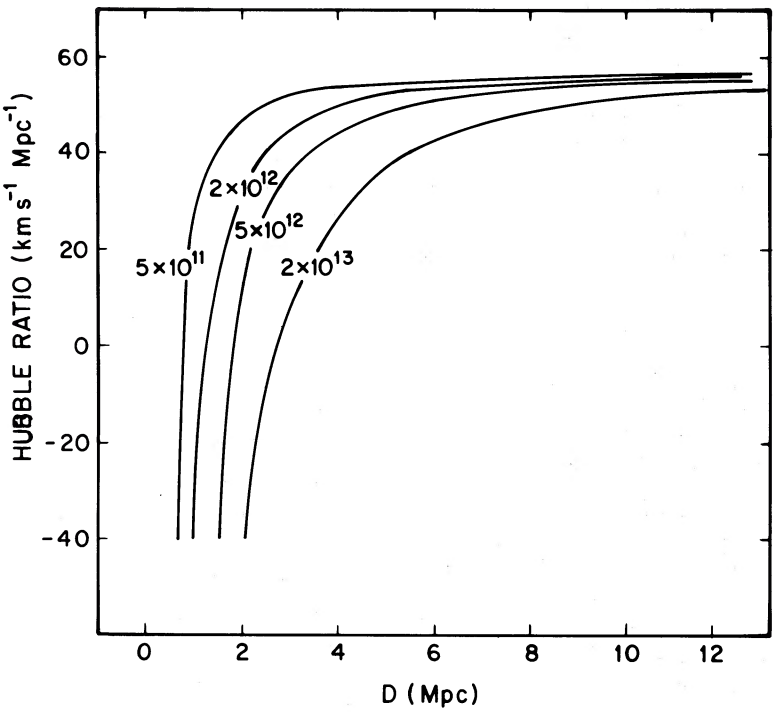

FIG. 4.—Predicted variation of the apparent Hubble v/r ratio with distance due to the deceleration caused by the Local Group for four assumed masses

to give values that would be observed in a zero force field. These corrections are calculated from equation (14), or its equivalent hyperbolic form, subtracted from the linear relation $v_H = H_0 r$. The sense of the plotted correction is the velocity to be added to the observed values so as to eliminate the deceleration due to the Local Group.

The correction reaches values greater than 300 km s^{-1} for distances less than 2 Mpc for the largest mass of $2 \times 10^{13} M_\odot$ considered. The corrections are smaller than 100 km s^{-1} for $r > 1$ Mpc if $M_{LG} = 5 \times 10^{11}$ or $2 \times 10^{12} M_\odot$.

The variation of the apparent Hubble ratio v/r is shown in Figure 4, calculated from equations (13) and (14) or their equivalent hyperbolic forms. The increase of v/r with distance is appreciable over distances as large as 10 Mpc for the $2 \times 10^{13} M_\odot$ massive case, but is much smaller for the two lowest masses, rising to $H = 40$ km s^{-1} Mpc^{-1} at 2.4 Mpc for $M_{LG} = 2 \times 10^{12} M_\odot$ and to $H = 50$ km s^{-1} Mpc^{-1} at a distance of 4 Mpc for the same mass, compared with the far-field value of $H_0 = 55$ km s^{-1} Mpc^{-1}.

d) Position of the Zero-Velocity Surface at the Present Epoch

Lynden-Bell (1981) has shown that the mass of the Local Group could be obtained in the absence of random velocities by locating the surface that separates expansion from contraction at the present epoch. This is not the surface of zero energy, but that of zero velocity *now*. That surface will move outward with time, but since we must specify the particular time of the present epoch to obtain the observed value of $H_0(r \to \infty)$, such a surface exists now in the region of negative energy and can be calculated from equations (13) and (14) at our particular epoch, or more generally from equations (4), (5), and (8) at any arbitrary epoch.

At the zero velocity surface, $\theta = \pi$ from equation (8). Let the time when this happens be T. The energy of particles just reaching $\theta = \pi$ at this time is given by equation (5) as

$$-2E = (\pi G M T^{-1})^{2/3}, \tag{15}$$

which, when substituted into equation (4), gives

$$r_0^3 = 2^3 \pi^{-2} G M T^2, \tag{16}$$

which is equation (7) of Lynden-Bell (1981). The mass of the Local Group is then

$$M_{LG} = \frac{\pi^2 r_0^3}{8 G T^2}. \tag{17}$$

Equation (17) can be made more explicit by requiring that the calculations make $H(\infty)$ consistent with the observations. This is done in equations (12)–(14) which, by the same route as above that specifies the epoch T, gives

$$M_{LG} = 8.47 \times 10^{11} r_0^3, \tag{18}$$

where r_0 is the distance to the zero-velocity surface in megaparsecs, and the mass of the Local Group is in solar units. (The distance r_0 is where the curves in Fig. 2 cross the $v = 0$ line.)

If the random velocities of local galaxies were strictly zero, Lynden-Bell (1981) suggests this to be a method of finding M_{LG}, but if random velocities do exist or if there are large errors in the distances, r_0 cannot be found from a single galaxy. Nevertheless, by fitting the family of v, r curves of Figure 2 to the total data, any random component either in velocity or distance can be more nearly averaged out, and the method survives in principle.

III. THE OBSERVATIONAL DATA FITTED TO THE CALCULATED DECELERATIONS

a) The Basic Data Corrected with the Standard Solar Motion

The accuracy to which distances and velocities of nearby galaxies are known has increased since the early 1950s with the

© American Astronomical Society • Provided by the NASA Astrophysics Data System

1986ApJ...307....1S

return to the problem of Hubble's distance scale when the 200 inch telescope began operation. A fundamental improvement in the accuracy of the velocities began when 21 cm radio data were routinely obtained for galaxies, following the pioneering work of Roberts (see Roberts 1969, for a review) and Epstein (1964). Velocities of the local late-type galaxies are now generally known to accuracies of $\sim \pm 5$ km s^{-1}.

Improvement in knowledge of distances is less satisfactory because of recondite uncertainties in the Cepheid and the brightest star calibrations, due to uncertain photometry, and because of uncertainties in the internal absorption corrections in galaxies needed to reduce apparent to true distance moduli.

The data as we adopt them here are set out in Table 1. Column (2) gives the assumed true distance modulus taken from the sources in column (3) listed at the bottom of the table. Many of these distances are new since $\sim$1970, mostly from Cepheids, a few from brightest resolved stars, and the last two from supernovae of type I, calibrated via brightest stars. The distances in column (4), which follow from the moduli in column (2), are relative to the Sun at the origin.

The velocities listed in column (5) are the result of reducing the observed 21 cm heliocentric velocities to the local standard of rest for the solar neighborhood and then to the centroid of the Local Group using the second solution of Yahil, Tammann, and Sandage (1977, hereafter YTS). This solar motion relative to the centroid is adopted to be $\Delta v = 300 \cos \lambda$ km s^{-1}, where λ is the angle from any particular galaxy to the adopted apex at $l = 107° \pm 5°$ and $b = -8° \pm 4°$, similar to 300 cos A from $l = 90°$, $b = 0°$ adopted by Humason, Mayall, and Sandage (1956) following the calculation of Mayall (1946) and of Humanson and Wahlquist (1955).

The basic data in column (5) are from the large number of original velocity sources set out in detail by YTS in the notes to their Table 1. The largest error quoted for the measured 21 cm data for any entry is ± 10 km s^{-1}; most are less than ± 5 km s^{-1} for galaxies listed as individuals. However, the velocities given for the six *groups* in Table 1 (IC 342 gr, NGC 300 gr, NGC 2403 gr, M81 gr, M101 gr, and the NGC 253 gr) are based on mean values of the group members. The velocity differences of order $\sim$100 km s^{-1} between the members give larger errors for the values listed in column (5) than for the individual galaxies. The details are as follows.

The mean velocities, the velocity dispersions among the galaxies taken to be members, and the number of members in a group are respectively $\langle v \rangle = 242 \pm 76$ (1 σ) from 10 members of the IC 342 group (i.e., the Maffei group); $\langle v \rangle = 123 \pm 28$ (1 σ) from four members of the NGC 300 group; $\langle v \rangle = 234 \pm 73$ (1 σ) from five members of the NGC 2403 group; $\langle v \rangle = 250 \pm 106$ (1 σ) from six members of the M81 group; $\langle v \rangle = 354 \pm 83$ (1 σ) from 10 members of the M101 group; $\langle v \rangle = 272 \pm 36$ (1 σ) from five members of the NGC 253 group. The errors of these mean values are $\sim \sigma / n^{1/2}$ for any given group, and range between ± 14 and ± 43 km s^{-1}.

b) *Velocity Correction for the Virgo Perturbation*

The distances in Table 1 are large enough for some galaxies that the velocity perturbation due to the pull of the Virgo complex overdensity cannot be neglected. The linear approximation to the full Virgocentric flow model gives a correction velocity of

$$v_g = v_{vc}(x) + v_{vc}(\cos \theta - x)[1 - (x^2 - 2x \cos \theta + 1)^{-1}] , \quad (19)$$

where v_{vc} is the infall velocity of the centroid of the Local Group toward the Virgo core, x is the distance ratio of any

TABLE 1

OBSERVED AND CORRECTED VELOCITIES AND DISTANCES OF VERY LOCAL GALAXIES

Name (1)	$(m-M)_0$ (2)	Source (3)	D (Mpc) (4)	v_{CLG} (km s^{-1}) (5)	Δv_{Vir} (km s^{-1}) (6)	v^0_{Virgo} (km s^{-1}) (7)	$D_{2/3}$ (Mpc) (8)
M33	24.7	1	0.87	+68	0	+68	0.46
NGC 6822	23.95	2	0.62	+5	0	+5	0.76
M31	24.12	3	0.67	−14	0	−14	0.23
IC 1613	24.43	4	0.77	−67	0	−67	0.51
Peg Dwarf	27	5	2.51	+62	−12	+50	2.39
Leo A	26.0	5	1.58	−9	−3	−12	1.71
WLM	24.9	6	0.95	−6	0	−6	0.80
IC 5152	26	7	1.58	+5	+1	+6	1.71
Sextans A	26.2	8	1.74	+117	−3	−114	2.07
Sextans B	26.2	8	1.74	+133	−3	+130	1.90
IC 342 gr	29	9	6.31	+242	+57	+299	5.76
NGC 3109	26.0	10	1.58	+130	+10	+140	1.97
NGC 300 gr	26.1	11	1.66	+123	−10	+113	1.64
NGC 2403 gr	27.8	12	2.63	+234	+34	+268	3.25
M81 gr	28.8	13	5.75	+250	+48	+298	5.57
M101 gr	29.2	14	6.92	+354	+27	+381	6.88
M51	30	7	10.0	+546	+19	+565	10.02
NGC 253 gr	27.5	15	3.16	+272	−24	+248	2.99
Virgo	31.7	16	21.9	+967	+220	+1187	21.9
Fornax	32.1	17	26.3	+1486	−43	+1443	26.3

SOURCES.—(1) Sandage and Carlson 1983; Sandage 1983*a*; Freedman 1985. (2) Kayser 1967. (3) Baade and Swope 1963. (4) Sandage 1971. (5) Sandage 1986. (6) Sandage and Carlson 1985*b*. (7) Estimate from brightest stars. (8) Sandage and Carlson 1985*a*. (9) Arp and Sandage 1985 for NGC 1569. (10) Demers, Kunkel, and Irwin 1985. (11) Graham 1984. (12) Tammann and Sandage 1968; Sandage 1984*b*. (13) Sandage 1984*a*. (14) Sandage and Tammann 1974; Sandage 1983*b*. (15) Using source (11) and an estimated magnitude difference between NGC 300 and the NGC 253 group. (16) Sandage and Tammann 1982*a*, 1985. (17) Sandage and Tammann 1982*b*.

© American Astronomical Society • Provided by the NASA Astrophysics Data System

1986ApJ...307....1S

galaxy in question to the distance of the Virgo center, and θ is the angle on the plane of the sky between that galaxy and M87. Precise calculations using the full nonlinear equations (Schechter 1980) have been given by Kraan-Korteweg (1985) for a large sample of galaxies. For our purposes equation (19) is convenient, which is equation (2) of Schechter with the uniform Hubble expansion subtracted.

The angle from Virgo for each of the galaxies in our sample is taken from the Kraan-Korteweg (1985) catalog; the x values relative to Virgo are found from column (4) of Table 1, and the infall velocity v_{vc} is assumed to be 220 km s^{-1} following Tammann and Sandage (1985). The calculated corrections are listed in column (6) which, when applied to column (5), gives the corrected velocity in column (7). This is the velocity that would have been observed from the centroid of the Local Group if the Virgo complex did not exist. With this correction we are left, then, with only the velocity perturbation superposed on the ideal Hubble flow caused by the Local Group—the effect we seek.

c) *The Deduced Deceleration from the Observed Velocity-Distance Relation*

The 20 velocities and distances in Table 1 are plotted in Figure 5. The point for M31 is plotted, although, as explained later, the dynamics of the M31 + Galaxy system is different than for the massless satellite galaxies about the Local Group center of mass. The nondecelerated linear relation that passes through (0, 0) is shown for a Hubble constant of 55 km s^{-1} Mpc^{-1}.

Note three features of Figure 5. (1) *The velocity-distance relation holds quite locally*, for distances even as small as ~ 2 Mpc. This remarkable fact shows immediately that it is not spoiled even at a level of ~ 100 km s^{-1} by nonregular streaming motions in this very nearby region. (2) The same result, expressed differently, is that the mean deviation of the points about the line drawn in Figure 5 has a standard deviation of only $\sigma(v) = 61$ km s^{-1}—it is remarkably small. The true dispersion in velocity must, of course, be even smaller because there are errors in the distances at such a level that all of the scatter about any appropriate mean line could be due to that. We require errors in the distances of only of order $\sim \pm 20\%$ for the scatter to disappear. (3) The most important feature for our present problem is that the best fitting relation through the points that are closer than $D \lesssim 4$ Mpc does not pass through the (0, 0) origin but, in fact, has negative velocities for the majority of galaxies with $D < 2$ Mpc. We take this to be the suggestion of a deceleration of the expansion by the mass of the Local Group.

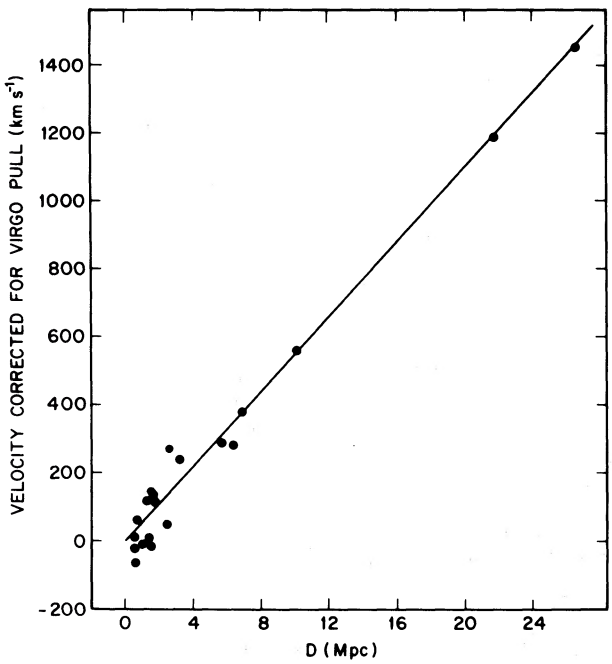

FIG. 5.—Corrected velocities and adopted distances for the 20 test objects listed in Table 1. The line is a linear relation passing through the origin with a slope of 55 km s^{-1} Mpc^{-1}.

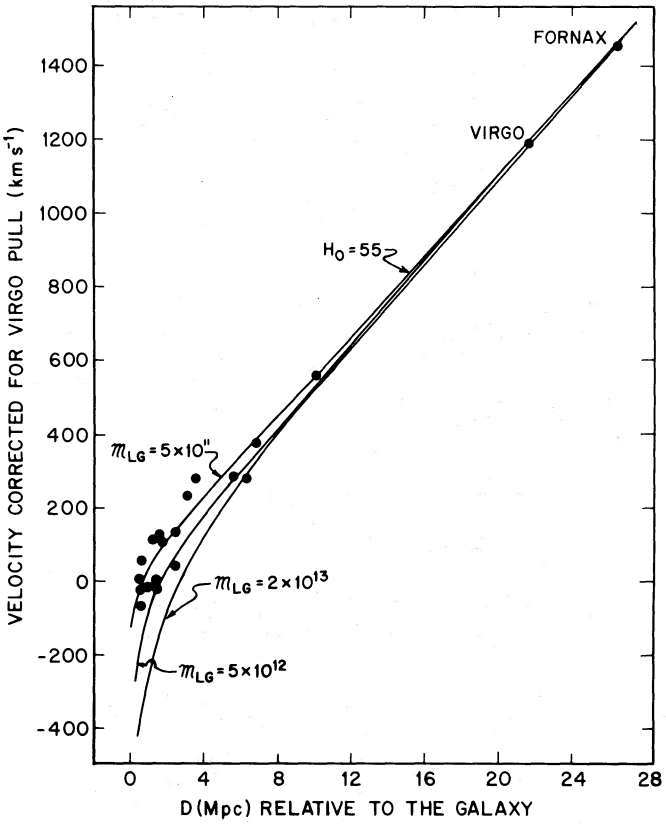

FIG. 6.—Data points of Table 1 compared with three of the predicted curves of Fig. 2 for Local Group masses of 5×10^{11}, 5×10^{12}, and 2×10^{13} $M_\odot$

The family of curves shown in Figure 2 is superposed on the data in Figure 6 to show that the expected effect, using the expected mass range of the Local Group, is consistent with the data. Three of the four calculated curves are shown for Local Group masses of 5×10^{11}, 5×10^{12}, and 2×10^{13} $M_\odot$.

d) *A Change of Origin*

None of the curves fit the data well. There is a large vertical disperson in the observed points in the distance range ~ 1.0–3 Mpc from the Sun. The *velocities* have been corrected to the centroid of the Local Group using solution (2) of YTS, and we test now if the scatter can be reduced by changing the origin of the *distances* to the centroid as well.

The mass ratio of M31 to our Galaxy is not well known, but is often taken to be $M_{M31}/M_G \approx 2$. The center of mass would then be on a line between the galaxies at two-thirds of the

© American Astronomical Society • Provided by the NASA Astrophysics Data System

1986ApJ...307....1S

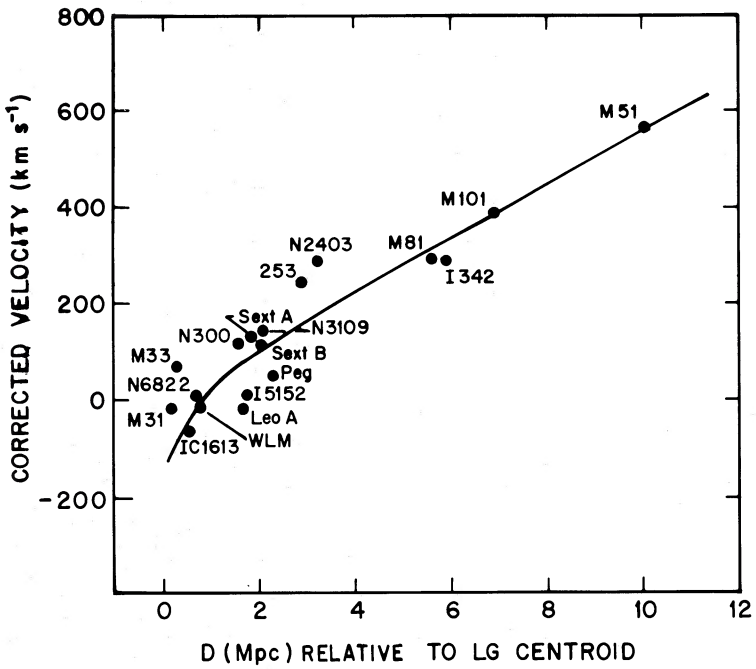

FIG. 7.—Observational data but with distances measured from a point on a line connecting the Galaxy and M31 at two-thirds the distance toward M31. The theoretical nonlinear velocity-distance relation for a Local Group mass of $5 \times 10^{11}\ M_\odot$ is shown.

distance to M31. We have transferred all distances to this new origin, with the result given in column (8) of Table 1.

e) The Adopted Deceleration and M_{LG} for the $\Omega_0 = 0$ Model

The data in columns (7) and (8) of Table 1 are plotted in Figure 7, which does, indeed, show a slight improvement over Figure 6 in the agreement between the calculations and the data. The single line in Figure 7 is the calculated velocity-distance relation for a Local Group mass of $5 \times 10^{11}\ M_\odot$ which, based on a minimum scatter of the residuals, is the best fit of the four calculated curves. (M31, although plotted in Figs. 5, 6, and 7 for reference, should be disregarded in the fit because this galaxy is not massless.)

A more quantitative comparison is made in Table 2 which lists the mean deviation $\langle \Delta v \rangle$ of the 17 points (with $D_{2/3} \leq 10$ Mpc calculated from the origin at the assumed centroid) from the calculated deceleration curves of Figure 2. The best-fit mass is $M_{LG} = 4 \times 10^{11}\ M_\odot$. Unacceptable fits begin for masses larger than $\sim 2 \times 10^{12}\ M_\odot$; a mass as large as $5 \times 10^{12}\ M_\odot$ is out of the question, as is shown also by Figure 6 directly.

TABLE 2

MEAN DEVIATION AND VELOCITY DISPERSION OF OBSERVED VELOCITY-DISTANCE DATA FROM PREDICTED CURVES FOR VARIOUS ASSUMED LOCAL GROUP MASSES FOR $H_0 = 0$ AND THE STANDARD CORRECTION FOR SOLAR MOTION

M_{LG} ($M_\odot$)	$\langle \Delta v \rangle$ (km s^{-1})	$\sigma\langle v \rangle$ (km s^{-1})
0	-16 ± 15	60.9
5×10^{11}	$+5 \pm 14$	56.4
2×10^{12}	$+35 \pm 14$	54.7
5×10^{12}	$+75 \pm 16$	64.4
2×10^{13}	$+198 \pm 30$	120.0

The standard deviation of the observed points about the five theoretical deceleration curves, read as velocity residuals, are in the third column. They are near $\sigma(v) \approx 60$ km s^{-1}, which is the same order as the deviation about the solar motion solution for the Local Group members alone (YTS 1977, Figs. 1–3).

As mentioned in § III*c*, this very small velocity dispersion is even more remarkable considering that appreciable errors must still exist in the adopted distances. We note in passing that estimates of the size of the one-dimensional random motion about the ideal Hubble expansion have, in fact, progressively decreased as the accuracy with which we claim to know distances to the test galaxies has increased. Hubble (1936) gave a value of $\sigma(v) = 200$ km s^{-1} for the random motion of local "field" galaxies whose redshifts are smaller than 1720 km s^{-1} (data from his Table V). He based this on residuals from a velocity-distance diagram for brightest resolved "stars" using his calibration of their absolute magnitude and an estimate of σ(Mpg) for these stars. Smaller values of $\sigma(v)$ for local field galaxies were obtained later by de Vaucouleurs (1958, Appendix) where he found $\sigma(v) \lesssim 100$ km s^{-1} for local "field" galaxies. Sandage and Tammann (1975, 1982*b*) found $\sigma(v) \lesssim 50$ km s^{-1}; Materne and Tammann (1976) gave $\sigma(v) \approx 50$ km s^{-1}; Rivolo and Yahil (1981) had $\sigma(v) \approx 90$ km s^{-1} for the three-dimensional value. Other values are reviewed elsewhere (Tammann and Sandage 1985), where it is emphasized that the apparent velocity dispersion of any sample increases as the size of the sampled region increases, due, undoubtedly, to the existence of systematic streaming motions (currents) rather than to virialized velocities.

Each of these studies depends on a particular method of distance determination. The question remains whether the real $\sigma(v)$ will approach zero as the distances become more accurately known, and this, of course, is one of the motivations for the present program on Cepheids and brightest stars in these very nearby galaxies (see Sandage and Carlson 1985*b* for a status report with earlier references).

© American Astronomical Society • Provided by the NASA Astrophysics Data System

1986ApJ...307....1S

Two points related to Figure 7 should now be made:

1. Hubble often emphasized that the "law of redshifts does not operate within the Local Group." Stated only in this form with no subsequent explanation, the phenomenon appears even more mysterious than it already is because it suggests that, whatever its cause, there is a local region free from the effect and, suddenly, at some distance (perhaps r_0 used here) the redshift effect begins. There is, of course, no mystery of a "shielded region"; rather the Local Group is a very restricted locale dominated by two massive galaxies where, over a range out to r_0 at the present epoch and to a somewhat greater distance in the future, the galaxies in this neighborhood have negative velocities caused by the pull of the Local Group and are falling back to form an even tighter Local Group. This concept of the turnaround was first used by Kahn and Woltjer (1959) in their fundamental paper on the origin of the Local Group where they explored the consequences of the fact that M31 is approaching the Galaxy—it either has turned around (leading to their famous timing argument), or part of the velocity of approach is due to random velocities of unknown origins.

2. The Kahn-Woltjer argument and all later variations and amplifications of it require that we know the correction to be applied to the observed M31 velocity relative to the local standard of rest of -298 ± 2 km s^{-1} to reduce it to a *relevant* reference frame, i.e., corrected for the solar motion relative to such a relevant frame. What is that frame?

Some authors correct only for the motion of the Sun about the center of the Galaxy using $v_{\rm rot}$ values between 220 and ~ 260 km s^{-1}. This gives a large (i.e., ~ 100 km s^{-1}) velocity of approach of M31 to the Galaxy. This, in turn leads to a large mass for the Local Group, generally in the range $3\text{–}6 \times 10^{12}$ $M_\odot$ (Kahn and Woltjer 1959; Einasto and Lynden-Bell 1982).

So far in this discussion, we have adopted here the high solar motion of the centroid *of the Local Group* of 300 km s^{-1} required by the dipole solution (which requires no knowledge of distances) relative to very local galaxies (YTS 1977, Figs. 1–3). The amplitude of the dipole signal is so large as to give a very *small* residual velocity of -14 km s^{-1} for M31 relative to the origin which we consider to be rlevant to the problem, but then, of course, with the consequence of a high value of the motion of the center of our Galaxy relative to the centroid, a point we have not yet considered. To rediscuss the Kahn-Woltjer calculation, the question of the solar motion must be approached directly because we must use it to determine the velocity of approach of M31 and the Galaxy. A new solution for the solar motion consistent with the dynamical model we are considering is the subject of the next section.

IV. SECOND APPROXIMATION TO THE VELOCITY CORRECTIONS USING A CONSTRAINED NEW SOLUTION FOR THE SOLAR MOTION

a) The Method

We now take seriously the model of Friedman big-bang dynamics with zero angular momentum extending into the Local Group. Because M31 and our Galaxy constitute virtually the total mass, the centroid of the Local Group must lie on the line between them. Furthermore, M31 and the Galaxy must move exactly toward each other, the center of mass being stationary. This means that the motion of the center of the Galaxy must point directly toward M31 at $l = 121°, b = -22°$. The solar motion relative to the Local Group centroid is the sum of the two vectors of Galactic rotation toward $l = 90°$, $b = 0°$ and the motion of the center of the Galaxy toward $l = 121°, b = -22°$.

Define the three vectors to be $\boldsymbol{A}$, the Sun's orbital velocity about the Galactic center; $\boldsymbol{C}$, the motion of the Galaxy toward M31; and $\boldsymbol{B}$, the sum of $\boldsymbol{A}$ and $\boldsymbol{C}$, which then is the solar motion relative to the Local Group centroid. (In the vector algebra we shall neglect the spatial offset of the Sun from the Galactic center.)

We are not totally without knowledge of the size and direction of these vectors. The quantity $\boldsymbol{B}$ is the vector solved for in the usual determinations of the solar motion relative to the Local Group. The value adopted in the last section was $|\boldsymbol{B}| = 300$ km s^{-1} toward $l = 107°, b = -8°$. The quantity $|\boldsymbol{A}|$ lies between 200 and 300 km s^{-1} and is constrained to be toward $l = 90°, b = 0°$. The first thing to note is that, taking solution (2) of YTS for $\boldsymbol{B}$ as above, and $\boldsymbol{A} = (0, 220, 0)$, gives $\boldsymbol{C} = (-87, +64, -42)$, where the unit vectors are $\boldsymbol{i}$ toward $l = 0, b = 0$, $\boldsymbol{j}$ toward $l = 90°, b = 0$, and $\boldsymbol{k}$ toward $b = 90°$. This direction of $\boldsymbol{C}$ is toward $l = 144°, b = -21°$—only 20° distant from the direction to M31 itself. Hence the condition that $\boldsymbol{C}$ be directed precisely toward M31 is approximately fulfilled even with the nonconstrained solution of YTS for $\boldsymbol{B}$.

We now require that $\boldsymbol{C}$ in fact points directly to M31 and find the conditions that this constraint puts on $|\boldsymbol{A}|$ (the absolute value of the Galactic rotation) and on $\boldsymbol{B}$. For any particular $|\boldsymbol{A}|$, $\boldsymbol{B}$ pair, the value of $|\boldsymbol{C}|$ is determined; hence, the size of the motion of the galactic center toward M31 is found.

The details of the vector algebra using $\boldsymbol{C} = \boldsymbol{B} - \boldsymbol{A}$ are straightforward. There is a unique value of $|\boldsymbol{C}|$ for given values of $|\boldsymbol{A}|$ and $|\boldsymbol{B}|$, and, furthermore, with $\boldsymbol{C}/|\boldsymbol{C}|$ known to be $(-0.478, +0.795, -0.375)$ from $l_c = 121°$, $b_c = -22°$, the direction cosines of $\boldsymbol{B}$ are found, giving the apex of $\boldsymbol{B}$, denoted by l_B, b_B.

The parameter space of $|\boldsymbol{A}|, |\boldsymbol{B}|, l_B, b_B$, and consequently $|\boldsymbol{C}|$, was explored letting $|\boldsymbol{A}|$ range between 220 and 320 km s^{-1}. The resulting $|\boldsymbol{C}|$ values ranged between 115 km s^{-1} and 0, and the resulting direction of $\boldsymbol{B}$ ranged between $100° \geq l \geq 90°$, $-8° < b \leq 0$, all reasonable values compared to what was known before. Hence the model *is* possible from the known data.

Once $\boldsymbol{B}$ is known, the angle θ between the direction of $\boldsymbol{B}$ and M31 is known. Now, since the observed velocity of M31 relative to the Sun is -298 km s^{-1} (YTS, Table 1), the peculiar velocity of M31 relative to the Local Group centroid is

$$v_{\rm M31}({\rm LG}) = |\boldsymbol{B}| \cos\theta - 298 \, . \tag{20}$$

The velocity of our Galaxy relative to the same centroid is $|\boldsymbol{C}|$. Hence the velocity of approach of the centers of M31 and the Galaxy is

$$v_{\rm M31} - v_{\rm G} = |\boldsymbol{C}| + |\boldsymbol{B}| \cos\theta - 298 \, , \tag{21}$$

which must, of course, equal $298 - |\boldsymbol{A}| \cos\phi$, where ϕ is the angle between $l = 90°$, $b = 0°$ and the direction of M31, which is $\phi = 37.^\circ3$. Hence, for any given value of $|\boldsymbol{A}|$ and $\boldsymbol{B}$, the velocity $|\boldsymbol{C}|$ of the Galaxy and the velocity $|\boldsymbol{B}| \cos\theta - 298$ for M31, both relative to the centroid of the Local Group, are known.

Now it is not *a priori* known what the exact value of $|\boldsymbol{B}|$ should be—all we know from the former, aforementioned, solutions of the solar motion is that it must be ~ 300 km s^{-1}. We proceed then as follows.

1. Adopt a value of $|\boldsymbol{A}|$.

© American Astronomical Society • Provided by the NASA Astrophysics Data System

1986ApJ...307....1S

2. Compute a series of l_B, b_B, and $|C|$ values for a series of adopted $|B|$ values in the range $220 \leq |B| \leq 320$ km s^{-1}.

3. From these, compute a series $|C|$ and v_{M31} values, for every $|B|$ value.

4. Repeat the process for other $|A|$ values in the range $220 \leq |A| \leq 260$ km s^{-1}.

In that way, for any $|A|$ value, from equation (21), which is equal to $|A| \cos \phi = 0.795\ |A|$, we obtain the velocity of approach of M31 to the Galactic center and a series of values of v_{M31} and v_G separately.

As $|B|$ is varied for any given $|A|$, the ratio of v_{M31}/v_G changes. Because the linear momentum of the M31 + Galaxy system must remain constant, there is a fixed value of v_{M31}/v_G for all time, although we do not know it until we know the mass ratios. On the two assumptions of $M_{M31} = M_G$ and $M_{M31} = 2M_G$, the $|B|$ and $|C|$ values can be obtained in the manner just described.

b) *Results and Application to the Basic Data*

The results of the vector algebra on $|A|$, B, and C are shown in Figure 8, taken from the summary of the calculations in Table 3. Plotted as abscissa is the Galactic rotation $|A|$. The bottom panel gives the relative velocity of approach of M31 and the Galaxy, being $298 - 0.795|A|$. As $|A|$ is varied between 220 and 260 km s^{-1}, this velocity decreases from 123 to 91 km s^{-1}. The middle panel shows the value of the motion of the Galactic center relative to the Local Group centroid $|C|$, for the two assumptions on the mass ratio. The top panel gives the value of $|B|$, again for two mass ratios.

It is the solution for B, i.e. $|B|$ and its direction, that is needed in Figures 5–7 to change the observed heliocentric velocities to those in the relevant Local Group frame. Figure 8 gives the range of permissible $|B|$ values; $|A|$ must certainly lie within the plotted range of $220 < |A| < 260$ km s^{-1}.

The previous formal solutions of $|B|$, summarized for example in YTS (1977, Table 1) with no constraint such as we have placed here, give some additional guide as to the value to adopt finally using Figure 8. With cognizance that the recent values of $|A|$ are near 220 km s^{-1} and $|B| \sim 300 \pm 20$ km s^{-1}, we have adopted the parameter values of $|A| = 230$ km s^{-1}, $|B| = 295$ km s^{-1}, which, with $v_G = 2v_{M31}$, requires the direction of B to be $l = 97°.2$, $b = -5°.6$. This is only $\sim 10°$ distant

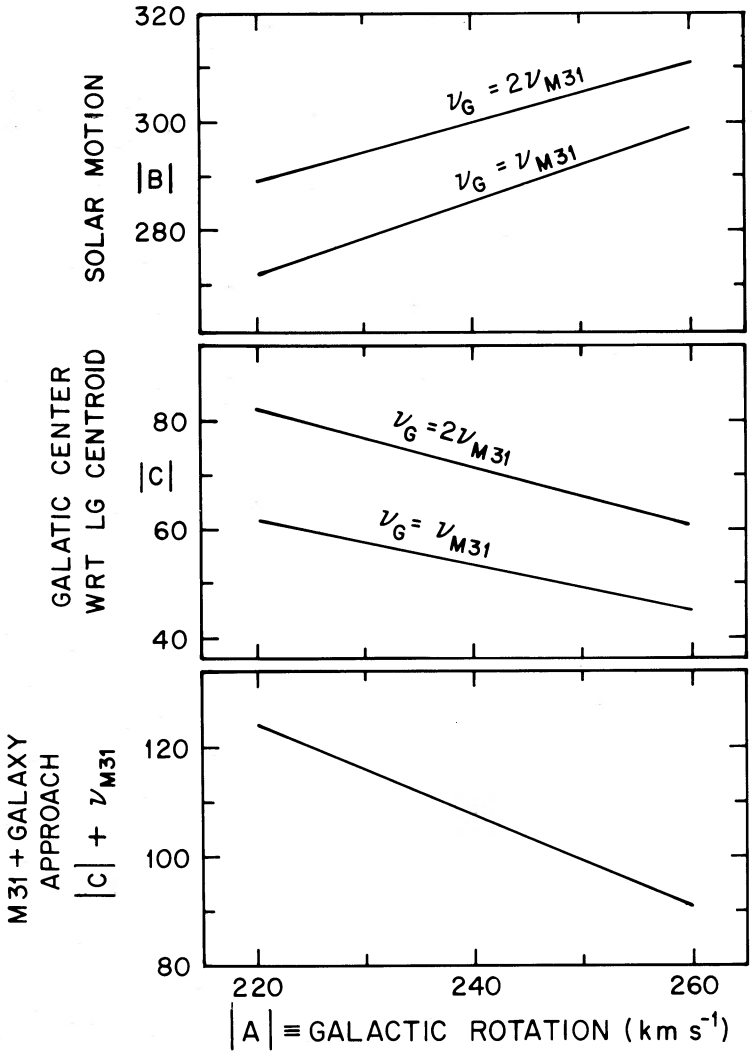

FIG. 8.—Summary of the Table 3 values of the dependences of $|B|$, $|C|$, and the velocity of approach of M31 and the Galaxy on the Galactic rotation velocity $|A|$. Two values of the mass ratio of the two galaxies are shown.

© American Astronomical Society • Provided by the NASA Astrophysics Data System

1986ApJ...307....1S

TABLE 3

SUMMARY OF DATA PLOTTED IN FIGURE 8 FOR THE EXPLORATION OF THE $|A|, B, |C|$ PARAMETER SPACE FOR TWO VALUES OF THE MASS RATIO

$\|A\|$ (km s^{-1}) (1)	$\|B\|$ (km s^{-1}) (2)	l_B (3)	b_B (4)	$\theta_{B,\mathrm{M31}}$ (5)	$\|C\|$ (km s^{-1}) (6)	$B\cos\theta - 298$ (km s^{-1}) (7)	M31 + Galaxy (km s^{-1}) (8)
For $v_G = 2v_{\mathrm{M31}}$							
220.....	289	97°.8	−6°.0	27.5	82	−42	124
230.....	295	97.1	−5.5	28.3	77	−38	115
240.....	300	96.6	−5.1	29.0	72	−36	108
250.....	305	95.9	−4.6	29.9	66	−33	99
260.....	311	95.4	−4.2	30.4	61	−30	91
For $v_G = v_{\mathrm{M31}}$							
220.....	272	96°.4	−4°.9	29.3	62	−62	124
230.....	281	95.6	−4.5	30.2	57	−57	114
240.....	285	95.0	−4.0	31.1	54	−54	108
250.....	290	94.5	−3.6	31.6	50	−50	100
260.....	299	94.2	−3.3	32.0	45	−45	90

NOTES.—The quantity $|A|$ is the magnitude of galactic rotation toward $l = 90°$, $b = 0$; $|B|$ is the solar motion relative to centroid of the Local Group in a direction l_B, b_B in cols. (3) and (4); $|C|$ is the velocity of the center of our Galaxy toward M31 at $l = 121°.2$, $b = -21°.6$ as seen from the Sun. Col. (7) is the motion of M31 toward the center of mass that is on a line between the center of M31 and the center of our Galaxy. The velocity of approach between our Galaxy and M31 is in col. (8). The angle between $\boldsymbol{B}$ and the direction of M31 is in col. (5).

from the solution (2) apex of YTS and is within the $\sim 2\,\sigma$ errors of the YTS solution with no constraints.

The solution gives the velocity of the Galactic center relative to the Local Group centroid to be -77 km s^{-1}, and $v_{\mathrm{M31}} = -38$ km s^{-1}, again approaching the centroid. The relative velocity of M31 toward our Galaxy (and vice versa) is then 115 km s^{-1}, in agreement with the lower panel of Figure 8.

The vector for the solar motion of $\boldsymbol{B} = (-36.8, +291.3, -28.8)$ is shown as the middle ridge line of the upper panel of Figure 9, where it is tested against the measured heliocentric velocities of the standard Local Group galaxies plotted versus the cosine of the angle between any given galaxy and the new apex at $l = 97°.2$, $b = -5°.6$. The data are listed in Table 4 which uses the same basic data as in Table 1, but now with the solar motion correction based on our new value of $\boldsymbol{B}$. The direction of $\boldsymbol{B}$ gives the cos θ values for each galaxy listed in column (5). The basic observed heliocentric velocity reduced to the local standard of rest is in column (6). The correction for solar motion is in column (7), and the correction for the Virgo pull in column (8), as previously calculated. Applying columns (7) and (8) to column (6) gives column (9) which, then, is the final corrected velocity relative to the centroid of the Local Group.

Previously recognized members of the Local Group have an asterisk to the left of column (1), and these are the 17 plotted points in the top panel of Figure 9. The ridge line at 295 cos θ is a satisfactory fit to the data, showing that our constrained solution for $\boldsymbol{B}$ does not violate these data. More distant galaxies from Table 4 are added in the bottom panel of Figure 9, showing, by the positive velocity residuals, the general cosmological expansion possessed by galaxies just beyond the Local Group.

Finally, the velocity-distance relation using these new corrected data for $\boldsymbol{B}$ from Table 1 is shown in Figure 10, which is the same as Figure 5 but uses Table 4 data rather than Table 1 data and with the new data for M31 and the Galaxy added as crosses. (The points for M31 and the Galaxy should be discounted *in the model fit* because the dynamics of two particles [with mass] moving on a rectilinear trajectory [their center of mass remaining stationary] is different from that of massless [satellite] particles moving relative to a stationary point at which the total mass remains stationary. The two crosses in Fig. 10 are then merely for reference. I am indebted to J. Ostriker for this fundamental point.) The 19 plotted points closer than Virgo are the first 19 entries in Table 4. The remaining entries are not plotted since they either have no fundamental distances (IC 10, DDO 187, DDO 210, GR 8), or they are clearly immediate satellites of the Galaxy. The reason they are listed in Table 4 is for their use in Figure 9, plotted as crosses.

V. COMPARISON OF THE $\Omega_0 = 0$ DECELERATION WITH THE DATA CORRECTED WITH THE NEW SOLAR MOTION

a) For $H_0 = 55$

The fit of the 19 galaxies in Table 4 with listed $D_{2/3}$ distances to the grid of calculated decelerations is shown in Figure 11. The model lines from Figure 2 are shown again for the five mass values of 0, 5×10^{11}, 2×10^{12}, 5×10^{12}, and 2×10^{13} $M_\odot$ for M_{LG} and with a time of 18.1×10^9 yr, which is $H_0 = 55$ km s^{-1} for $\Omega_0 = 0$. The conclusion is the same as discussed in § III, viz. the best fit is $M_{\mathrm{LG}} = 5 \times 10^{11}\ M_\odot$, but 2×10^{12} $M_\odot$ cannot be excluded at the $\sim 2\,\sigma$ level in the mean value of the residuals. The data for the mean deviations in Figure 11 are listed in Table 5, to be compared with Table 2.

b) For Different Values of H_0

The far-field data in Figure 11 for $D_{2/3} > 4$ Mpc (these are the M81 group, IC 342 group, M101, and M51) are consistent with $H_0 = 55$, but suppose we were to discount these four most distant points and ask what the family of predicted decelerations would be by changing the available time. This is equivalent to changing the value of H_0, again keeping $\Omega_0 = 0$. Keeping the Local Group mass the same, the decelerations will

© American Astronomical Society • Provided by the NASA Astrophysics Data System

1986ApJ...307....1S

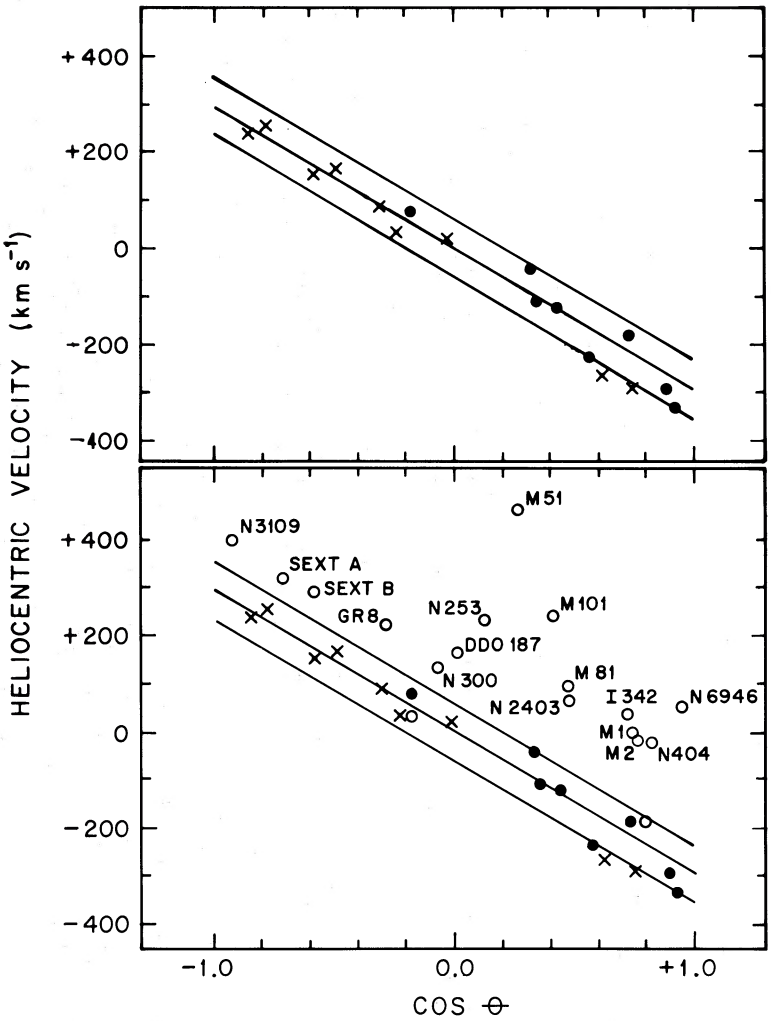

FIG. 9.—*Upper*: Galaxies in Table 4 with asterisks before col. (1). These are the adopted members of the Local Group. Closed circles are those galaxies that may move independently of the Galaxy. Crosses are satellites of the Galaxy which, nevertheless, follow the adopted constrained solar motion solution of 295 km s^{-1} toward $l = 97°.2, b = -5°.6$ shown as the center ridge line. Envelope lines are ± 60 km s^{-1} from the center line.

Lower: Same as above, but with the remaining galaxies in Table 4 plotted showing the expansion as the velocity residual from the center line read at a given cos θ value.

be different because the time over which we integrate the decelerations are now different. The formalism in § II can be applied again with different values of T to produce the predicted family of deceleration curves for $H_0 = 90, \Omega_0 = 0$ (or $T = 1.11 \times 10^{10}$ yr) in Figure 12, and $H_0 = 40, \Omega_0 = 0$ (or $T = 2.5 \times 10^{10}$ yr) in Figure 13. As mentioned, neither of these family of curves fit the far-field data, but never mind for this test, since we are interested in the effect on the nearby data closer than $D_{2/3} \approx 3$ Mpc.

As expected, for the short time scale of $H_0 = 90$ in Figure 12 the acceptable Local Group mass is now larger than in Figure 11. This is because over a shorter time available for the deceleration to occur, we must have a larger mass to produce the same effect as that caused by a smaller mass acting over a longer time. Figure 12 shows that a mass of $M_{LG} \approx 5 \times 10^{12}$ is the best fit to the 13 inner points.

The opposite conclusion for the same reason follows if $H_0 = 40$. Figure 13 shows the predicted family for this case. The fit to the data for the six most distant galaxies is poor. The remaining 13 points are best fit by $M_{LG} \sim 3 \times 10^{11} M_\odot$.

We emphasize that interesting as these results are, neither alternate value of H_0 is acceptable if we adopt the distance to M81 as $m-M = 28.8$ and $m-M$ to M101 as 29.2 as required by the Cepheid data, making Figure 11 with $M_{LG} \sim 5 \times 10^{11}$ $M_\odot$ the only viable solution.

VI. THE KAHN-WOLTJER TIMING ARGUMENT FOR M31 AND THE GALAXY

The first convincing evidence for appreciable dark matter in galaxies was Babcock's (1939) discovery of the large increase in M/L in the outer regions of M31 required by the flat rotation curve he measured. The argument was extended to the total gravitational field of M31 plus the Galaxy by Kahn and Woltjer (1959), who introduced the basic argument used so far in this paper. We repeat their argument using the present formalism and the new data for the velocity of approach from § IV.

The basic equations are the same as in § II for the negative energy case. The known quantities are now r (distance between M31 and the Galaxy), T (time since the beginning), and v (the

© American Astronomical Society • Provided by the NASA Astrophysics Data System

1986ApJ...307....1S

TABLE 4

BASIC DATA CORRECTED FOR THE SECOND APPROXIMATION SOLUTION FOR THE SOLAR MOTION

Name	ℓ	b	$(m-M)_o$	cos θ^{Δ}	v_{LSR}	295 cos θ	ΔV_{vir}	V^v_{CLG}	$D_{2/3}$
(1)	(2)	(3)	(4)	(5)	(6)	(7)	(8)	(9)	(10)
*M31	121.2	-21.6	24.12	+0.881	-298	+260	0	-38	0.23
Galaxy	.....	.....	.....	.....	....	....	0	-77	0.44
*M33	133.6	-31.3	24.7	+0.735	-182	+217	0	+35	0.46
* IC 1613	129.9	-60.6	24.43	+0.574	-239	+169	0	-70	0.51
* NGC 6822	25.4	-18.4	23.95	+0.326	-48	+96	0	+48	0.76
*WLM	75.7	-73.6	24.9	+0.354	-119	+104	0	-14	0.80
NGC 300	299.2	-79.4	26.1	-0.073	+135	-22	-10	+103	1.64
Leo A	196.9	+52.4	26	-0.180	+24	-53	-3	-32	1.71
*IC 5152	343.9	-50.2	26	-0.177	+76	-52	+1	+25	1.71
Sextans B	233.2	+43.8	26.2	-0.584	+289	-172	-3	+114	1.90
NGC 3109	262.1	+23.1	26.0	-0.922	+394	-272	0	+122	1.97
Sextans A	246.2	+39.9	26.2	-0.717	+317	-212	-3	+102	2.07
Pegasus	94.8	-43.5	27	+0.789	-178	+233	-12	+43	2.39
NGC 253	97.6	-88.0	27.5	+0.133	+232	+39	-24	+247	2.99
NGC 2403gr	150.6	+29.2	27.8	+0.470	+67	+139	+34	+240	3.25
M81gr	142.1	+40.9	28.8	+0.469	+94	+138	+48	+280	5.57
IC 342gr	138.2	+10.6	29	+0.80	+6	+237	+57	+294	5.76
M101	102.1	+59.8	29.2	+0.414	+241	+122	+27	+390	6.88
M51	104.9	+68.6	30.0	+0.269	+464	+79	+19	+562	10.02
*SMC	302.8	-44.3	....	-0.574	+154	-169	0	-15	....
*LMC	279.3	-33.4	....	-0.776	+257	-229	0	+28	....
*IC 10	119.0	-3.3	....	+0.928	-337	+274	0	-63	....
DDO 187	25.6	+70.5	....	+0.012	+164	+3	0	+167	....
*DDO 210	34.1	-31.3	....	+0.436	-123	+129	0	+6	....
GR8	310.7	+77.0	....	-0.282	+223	-83	0	+140	....
*Draco+	86.4	+34.7	....	0.748	-291 ± 6	+221	0	-70	....
*UMi+	105.0	+44.8	....	0.630	-261 ± 6	+186	0	-75	....
*Sculptor+	287.8	-83.2	....	-0.018	+20 ± 22	-5	0	+15	....
*Fornax	237.3	-65.7	....	-0.225	+36 ± 10	-66	0	-30	....
*Carina+	260.1	-22.2	....	-0.843	+240 ± 10	-249	0	-9	....
*Leo I+	226.0	+49.1	....	-0.482	+168 ± 40	-142	0	+26	....
*Leo II+	220.1	+67.2	....	-0.300	+90 ± 40	-88	0	+2	....
NGC 404	127.0	-27.0	....	0.814	-22	240	...	....	....
NGC 6946	95.7	+11.7	....	0.954	+54	281	...	....	....
IC 342	138.2	+10.6	....	0.720	+34	202	+57	294	....
Maffei 1	136.1	-0.2	....	0.774	-8	228	...	±26	....
Maffei 2	136.9	0.0	....	0.766	-15	226	...	....	....

[Δ] The angle θ is from the adopted solar motion apex at $l = 97°.2$, $b = -5°.6$.
[†] Velocities relative to Sun from the listing by Lynden-Bell, Cannon, and Godwin 1983.
* Adopted members of the Local Group.

velocity of approach). The equations for these quantities are (4), (5), and (8) which contain the three unknowns of $-2E$, GM, and θ, where M is now the sum of the masses of M31 and the Galaxy. In the calculation it is convenient to eliminate $-2E$ from the equations to retain two parametric equations containing θ and M.

TABLE 5

MEAN DEVIATION AND VELOCITY DISPERSION OF OBSERVED VELOCITY-DISTANCE DATA FROM PREDICTED CURVES FOR VARIOUS LOCAL GROUP MASSES FOR $\Omega_0 = 0$ USING THE NEW CONSTRAINED SOLUTION FOR THE SOLAR MOTION

M_{LG} ($M_\odot$)	$\langle \Delta V \rangle$ (km s^{-1})	$\sigma(V)$ (km s^{-1})
0	-42 ± 15	51
5×10^{11}	$+4 \pm 16$	56
2×10^{12}	$+53 \pm 21$	73
5×10^{12}	$+127 \pm 29$	102
2×10^{13}	$+289 \pm 46$	152

Combining equations (4) and (5) to eliminate $-2E$ gives

$$r^3 = \frac{GMT^2(1 - \cos\theta)^3}{(\theta - \sin\theta)^2}. \tag{22}$$

Combining equations (5) and (8) also to eliminate $-2E$ gives

$$T = \frac{v^3 r^3}{(GM)^2} \frac{(\theta - \sin\theta)}{(\sin\theta)^3}. \tag{23}$$

Rather than eliminating θ from equations (22) and (23) to retain M as the only unknown, it is easier to solve for θ and then for M parametrically. Combining equations (22) and (23) gives

$$\frac{r}{vT} = \frac{(1 - \cos\theta)^2}{\sin\theta(\theta - \sin\theta)}. \tag{24}$$

Because r, v, and T are known, θ can be found from equation (24), from which with either equation (22) or (23) M can be found.

© American Astronomical Society • Provided by the NASA Astrophysics Data System

1986ApJ...307....1S

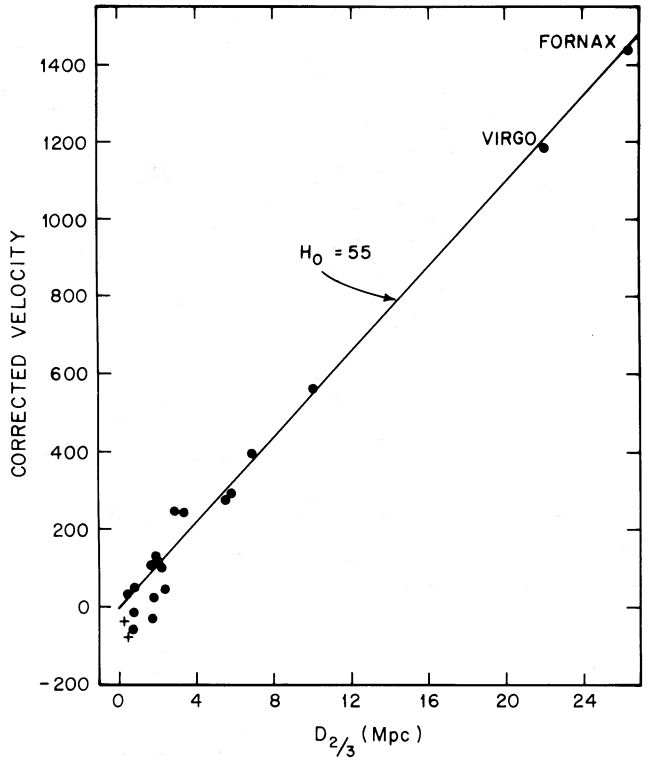

FIG. 10.—Data of observation corrected for the new solar motion, from Table 4. The line is for $H_0 = 55$ with no deceleration, passing through 0, 0.

From the new value of $\boldsymbol{B}$ in § IV we adopt the data for the M31, Galaxy pair to be

$$v = -115 \text{ km s}^{-1} \text{ approach}, \qquad r = 0.67 \text{ Mpc}$$

$$T = 18.1 \times 10^9 \text{ yr}.$$

These values in equation (24) give

$$\theta = 4.4294 \text{ rad},$$

which in equation (22) or (23) gives

$$M_{\text{M31+G}} = 2.9 \times 10^{12}\, M_\odot \tag{25}$$

for the combined mass.

Figure 8 or Table 3 shows that the smallest velocity of approach that is reasonable is -91 km s^{-1} for $|\boldsymbol{A}| = 260$ km s^{-1} and $|\boldsymbol{B}| = 311$ km s^{-1} (the rotational velocity at the solar circle can hardly be larger than 260 km s^{-1}). With this smallest approach speed the same calculation gives $\theta = 4.3131$ rad, and

$$M_{\text{M31+G}} = 2.1 \times 10^{12}\, M_\odot . \tag{26}$$

If the time is made shorter, the mass increases, because, as before, to reach the same dynamical state in a shorter time requires a bigger effect. For example, if $H_0 = 50$ but $\Omega_0 = 1$, then $T = 2/3H_0^{-1} = 13.1 \times 10^9$ yr, and equations (22) and (24) combine to give $M_{\text{M31+G}} = 3.6 \times 10^{12}\, M_\odot$.

Our most likely Kahn-Woltjer value, using $v = -115$ km s^{-1}, of $M_{\text{tot}} = 2.9 \times 10^{12}\, M_\odot$ is larger by a factor of 7 than $4 \times 10^{11}\, M_\odot$ given by the deceleration data for the entire sample, suggesting that the M31 approach is not caused entirely by the mutual attraction or indeed that M31 and the Galaxy may not be bound (Burbidge 1975), and therefore that these galaxies are merely passing in the night with at least a component of a random velocity due to an unknown initial condition. In this case, the method of §§ II–III would give the correct answer rather than the Kahn-Woltjer method for the total mass of the Local Group if the total random motions cancel in Figures 5–7 and 11–13.

That there may indeed be a random initial condition velocity to the M31-Galaxy system in addition to the dynamical infall velocity calculated by the method is suggested by con-

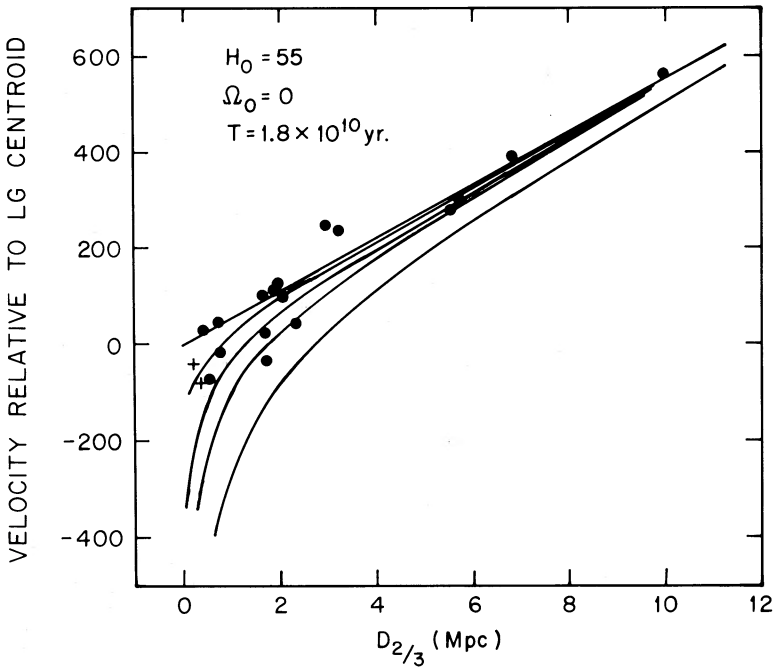

FIG. 11.—Data of Fig. 10 (Table 4) compared with the model predictions of Fig. 2 for $H_0 = 55$, $\Omega_0 = 0$. The five curves are for Local Group masses of 0, 5×10^{11}, 2×10^{12}, 5×10^{12}, and $2 \times 10^{13}\, M_\odot$.

© American Astronomical Society • Provided by the NASA Astrophysics Data System

1986ApJ...307....1S

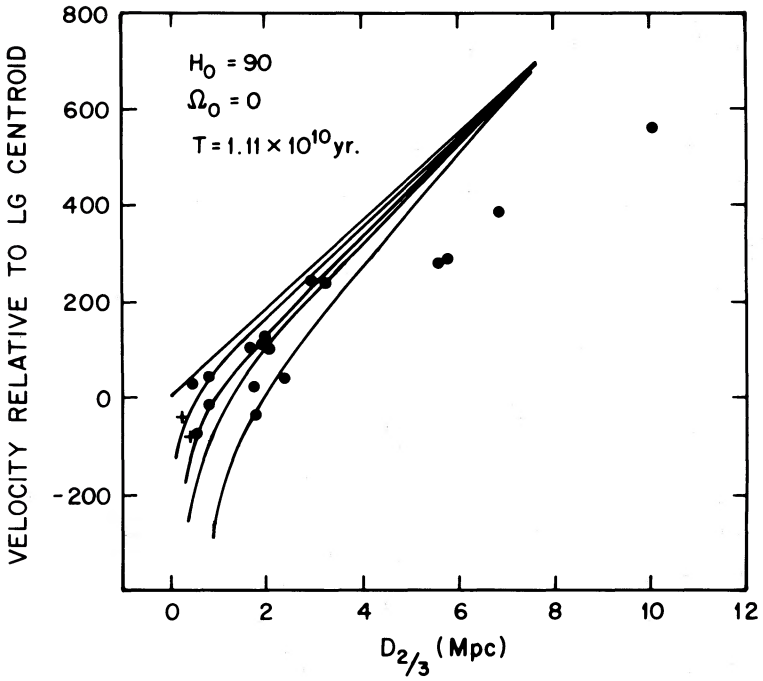

FIG. 12.—Same data as Fig. 11, for $H_0 = 90$

sidering the size of the random velocity of Local Group members, shown in Figure 10 as $\sigma(\mathrm{LG}) = 60$ km s^{-1}. If this is a virial velocity dispersion, the Local Group mass is

$$M_{\mathrm{LG}} \sim \sigma^2 r/G ,$$

which, if $r = 0.5$ Mpc, gives $4 \times 10^{11}\ M_\odot$, again smaller than the Kahn-Woltjer value, showing that -115 km s^{-1} (approach) is too high.

VII. DECELERATION OF THE LOCAL GALAXIES IN A SPACE WITH $\Omega_0 = 1$

It now only remains to consider the problem of particles injected into a space where matter is uniformly distributed between the galaxies in such amounts that the mean density is any arbitrary value $\langle\rho\rangle$. It can be shown that as long as $\langle\rho\rangle$ is not a function of r the velocity–distance relation is strictly linear no matter how high $\langle\rho\rangle$ may be, provided there is no

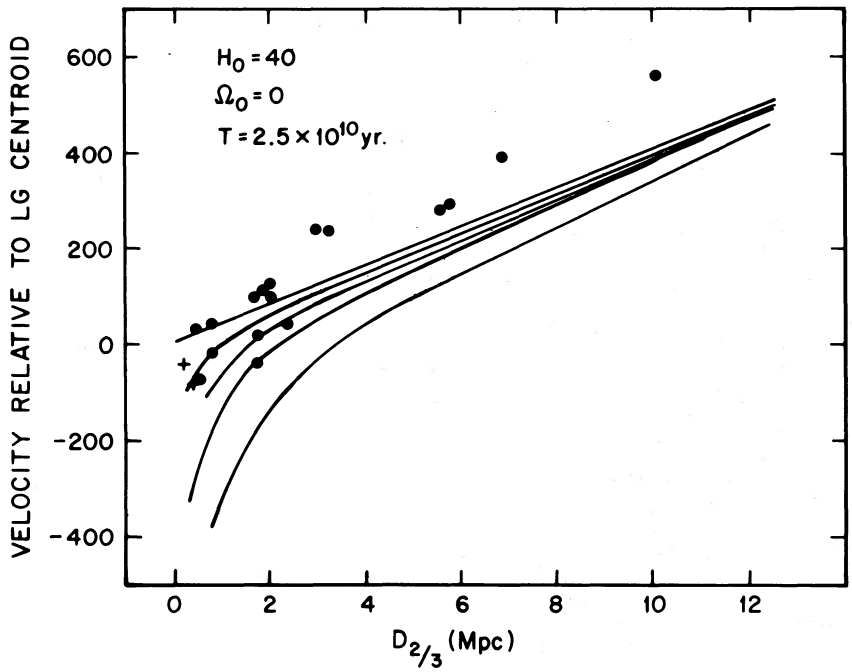

FIG. 13.—Same data as Fig. 11, for $H_0 = 40$

© American Astronomical Society • Provided by the NASA Astrophysics Data System

1986ApJ...307....1S

additional central mass M_{LG} to the Local Group. The relation becomes nonlinear in the manner of Figure 2 only if a central mass M_{LG} is introduced in addition to $\langle\rho\rangle$, and we wish to calculate its effect.

We assume that the uniformly distributed matter moves with the same Hubble expansion as the galaxies. Hence, the mass interior to any radius r from the center of the LG is constant for all time regardless of the form of $r(t)$. This total mass interior to r is

$$M_T(r) = M_{LG} + \tfrac{4}{3}\pi r^3\langle\rho\rangle \, . \tag{27}$$

From the standard result of Newtonian cosmology

$$\langle\rho\rangle = \frac{3H_0^2}{4\pi G} q_0 \, , \tag{28}$$

where, if $\Lambda = 0$, then $\Omega_0 = 2q_0$ and

$$\langle\rho\rangle = \frac{3H_0^2}{8\pi G} \Omega_0 \, , \tag{29}$$

where we make the usual distinction that q_0 is a measure of the intrinsic spacetime geometry of the manifold and Ω_0 is a measure of the density.

The value of H_0 is specified by the observations, and for any given value of Ω_0, the time T since the beginning is found from the time scale equations that give $T = f(q_0)H_0^{-1}$ (see Sandage 1961*a*, Table 8). If $\Omega_0 = 1$, then $T = 2/3H_0^{-1}$ for the flat spacetime case. Although there is no observational evidence now to support such a high value of Ω_0, we adopt this extreme case here to explore the consequences of a high density outside space.

The calculation of the deceleration is now the same as before, except that for every r we must use the $M_T(r)$ value for the mass inside r given by equation (27). Because we must specify r at the onset of the calculation so as to use the correct M_T, equations (22) and (24) are naturally suited to obtain the required velocity distance relation.

For this example we assume $H_0 = 55$, $\Omega_0 = 1$, hence $T = 2/3H_0^{-1} = 11.9 \times 10^9$ yr, and $\langle\rho\rangle = 8.39 \times 10^{10}$ solar masses per Mpc^3. The calculation begins by assuming various r values from which $M_T(r)$ follows from equation (27) for any assumed M_{LG} value. The known values of r, T, and M_T in equation (22) gives θ, which when put into

$$v = \frac{r}{T}\frac{\sin\theta(\theta - \sin\theta)}{(1 - \cos\theta)^2} \, , \tag{30}$$

which is equation (24), gives the required velocity v. In this way the v, r relation is built up for any desired value of r. The process is repeated for different M_{LG} values to produce a family of deceleration curves.[2]

The result is shown in Figure 14 with the data points from Table 4 superposed. The five curves are again for Local Group masses of 0, 5×10^{11}, 2×10^{12}, 5×10^{12}, and 2×10^{13} solar masses. The curves are similar to the $\Omega_0 = 0$, $H_0 = 55$ case of Figures 2 and 11; this is not surprising because, although the time scale is shorter for the $\Omega_0 = 1$ case than for empty space (two-thirds as long), the mass interior to r is larger by the second term in equation (27). By the argument given before, viz. that to obtain the same deceleration one needs a larger mass if it operates over a shorter time, one understands why Figures 2 and 14 are so similar because of the combination of a larger mass and a shorter time in the $\Omega_0 = 1$ case. But the $\Omega_0 = 0$ and $\Omega_0 = 1$ models are not identical. The summary in

[2] Using this procedure it is instructive to calculate the v, r relation for $M_{LG} = 0$ to show from eqs. (22) and (24) that $\theta = 0$ for all r, that then $\sin\theta(\theta - \sin\theta)/(1 - \cos\theta)^2 = \frac{2}{3}$ for all r, and hence from equation (30) that

$$v = \tfrac{2}{3}rT^{-1} \equiv H_0 r \, ,$$

as must hold for this special $\Omega_0 = 1$ case.

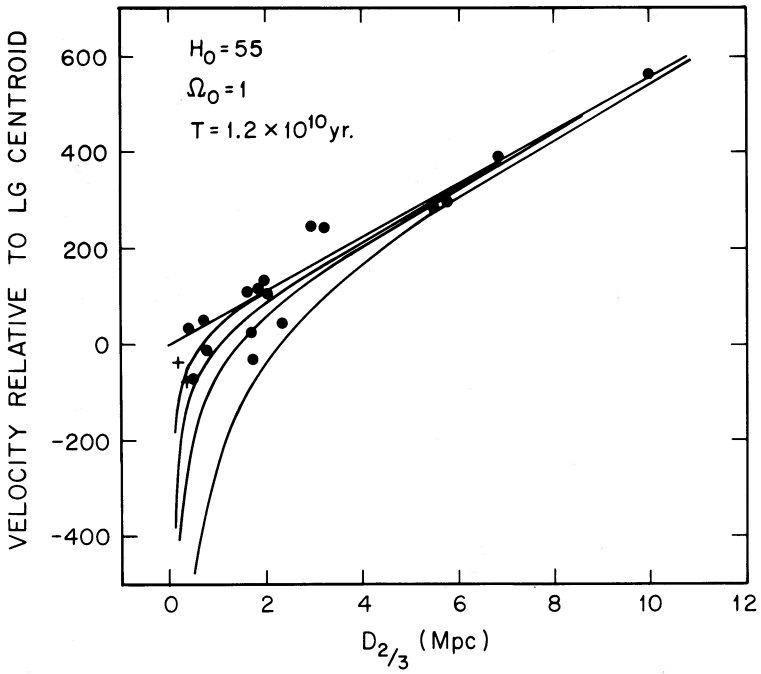

FIG. 14.—Same data as Fig. 11, for the theoretical decelerations for $H_0 = 55$ in a space with $\Omega_0 = 1$

© American Astronomical Society • Provided by the NASA Astrophysics Data System

1986ApJ...307....1S

TABLE 6

MEAN DEVIATION AND VELOCITY DISPERSION OF OBSERVED VELOCITY-DISTANCE DATA FROM PREDICTED CURVES FOR VARIOUS LOCAL GROUP MASSES FOR $\Omega_0 = 1$ USING THE NEW CONSTRAINED SOLUTION FOR THE SOLAR MOTION

M_{LG} ($M_\odot$)	ΔV (km s^{-1})	$\sigma(v)$ (km s^{-1})
0	-42 ± 15	51
5×10^{11}	-12 ± 16	55
2×10^{12}	$+36 \pm 23$	78
5×10^{12}	$+101 \pm 33$	113
2×10^{13}	$+246 \pm 48$	159

Table 6 of the residuals of the observations from the calculated curves shows a difference from Table 5. From Table 6 we deduce that the best-fit value of the Local Group mass is

$$M_{LG}(\Omega_0 = 1) = 8 \times 10^{11}\ M_\odot\ , \tag{31}$$

which is higher than the Table 5 value of

$$M_{LG}(\Omega_0 = 0) = 4 \times 10^{11}\ M_\odot\ . \tag{32}$$

From the size of the errors on the residuals of $\langle \Delta V \rangle$ in both Tables 5 and 6, the 1 σ errors on these mass values is a factor of ~ 2. But because the $\Omega_0 = 1$ case has no observational justification from all known cosmological tests (see Sandage and Tammann 1983, 1986), we adopt the equation (32) value of $4 \times 10^{11}\ M_\odot$ as the best mass determination via the local galaxy data. Comparison with other values is made in the next section.

VIII. MASS-TO-LIGHT RATIO AND COMPARISONS WITH OTHER MASS DETERMINATIONS

With the introduction of a "slightly" massive halo to our Galaxy that was thought to be necessary to stabilize the cold galactic disk (Ostriker and Peebles 1973), the notion of *very* massive halos attached to disk galaxies has grown. Whereas the ratio of halo-to-disk mass needed for disk stability is only ~ 2.5 in the Ostriker-Peebles N-body simulations, much heavier halos were introduced (Einasto, Kaasik, and Saar 1974; Ostriker, Peebles, and Yahil 1974) for a variety of other dynamical reasons, leading to mass-to-light ratios of the order of ~ 100. This would give a total mass per giant spiral galaxy such as M31 of $\sim 7 \times 10^{12}\ M_\odot$ which is a factor of ~ 20 larger than the value in equation (32).

Many attempts have been made either to build models of the mass distribution of our Galaxy with such a massive halo (see Ostriker and Caldwell 1983 for a review of the literature to 1982), or to determine the total mass of the Galaxy at large distances using measured radial velocities of satellite objects in the high halo (see Hartwick and Sargent 1978; Bahcall and Tremaine 1981; Hawkins 1983). These studies gave some support to the conjecture of a massive halo, albeit each with the caveat of considerable uncertainty due to the large errors in the observed velocities.

A very early critic of the first discussions was Burbidge (1975), who concluded from a number of arguments that the mass of the Galaxy out to 70 kpc was not more than 2×10^{11} $M_\odot$. Similar conclusions have more recently been reached by Miyamoto, Satoh, and Ohashi (1980) and by Wakamatsu (1981). A contrary conclusion was reached by Innanen, Harris, and Webbink (1983).

As the observational data on velocities improved, the early direct evidence for a very massive halo to our Galaxy has slipped (see Lynden-Bell and Lin 1977; Lin and Lynden-Bell 1977). The most recent discussions by Lynden-Bell, Cannon, and Godwin (1983) yield a mass of the Galaxy out to 100 kpc of only $(2.6 \pm 0.8) \times 10^{11}\ M_\odot$. A further discussion by Suntzeff, Olszewski, and Stetson (1985) suggests an even smaller value of $1.8 \times 10^{11}\ M_\odot$ out to the distance of the remote globular cluster AM-1 (Lauberts 1976; Madore and Arp 1979) at a distance of 120 Mpc (Aaronson, Schommer, and Olszewski 1984). These numbers are similar to the mass of $2 \times 10^{11}\ M_\odot$ out to ~ 60 kpc for the giant galaxy NGC 3992 (of absolute magnitude $M^0_{B_T} = -21.8$) obtained by Gottesman and Hunter (1982), belying any massive halo of the order of $10^{12}\ M_\odot$ for that galaxy.

There are then, two limiting cases for the expected mass of the Local Group. The most conservative assumption is that M31 and the Galaxy have the same mass, each of $2 \times 10^{11}\ M_\odot$ for a total of $M_{LG} = 4 \times 10^{11}\ M_\odot$ – equal to our "best" value from the present deceleration method. If, on the other hand, we adopt an M/L ratio of 100 advocated by Einasto, Kaasik, and Saar (1974) and Ostriker, Peebles, and Yahil (1974), and put the luminosity of M31 equal to the Galaxy, each with $L_B = 7 \times 10^{10}\ L_\odot$ [i.e., the absolute magnitude of M31 is $M^0_{B_T} = -21.6$ and $M_B(\odot) = +5.5$], the total luminosity of M31 plus the Galaxy is $1.4 \times 10^{11}\ L_\odot$, and the total mass would then be $1.4 \times 10^{13}\ M_\odot$, an impossible value according to Figures 5, 6, 7, 11, and 14, and Tables 2, 5, and 6, because the expected deceleration for distances smaller than ~ 4 Mpc is too large by many σ. What then are the limits on M/L imposed by the smallness of the observed deceleration?

The total luminosity of the Local Group is closely the sum of M31, M33, and our Galaxy. Suppose, as in § III, that M31 has twice the mass (and hence twice the luminosity). In that case, $M^0_{B_T}(\text{M31}) = -21.61$, $M^0_{B_T}(\text{Galaxy}) = -20.86$. The luminosity of M33 is taken to be $M^0_{B_T} = -19.1$. The sum is $L_{LG} = 1.11 \times 10^{11}\ L_\odot$. The resulting M/L values are listed in the second column of Table 7. If, on the other hand, $L(\text{Galaxy}) = L(\text{M31})$, then $L_{LG} = 1.5 \times 10^{11}$, and the resulting M/L values are in column (3).

The conclusion from §§ III and V is that, although $M_{LG} = 4 \times 10^{11}\ M_\odot$ is the best value from the deceleration data, a mass as high as $2 \times 10^{12}\ M_\odot$ cannot be ruled out. On the other hand, values as high as 5×10^{12} are not possible with the present data. The conclusion is that our best value of M/L is 3; values as high as ~ 30 contradict the data. The principal conclusion is that we have no evidence from the deceleration method for a supermassive halo for either our Galaxy or for M31, no evidence from galaxies themselves that Ω_0 can even remotely approach the closure value of unity for the universe

TABLE 7

M/L VALUES OF THE LOCAL GROUP FOR FIVE ASSUMED TOTAL MASSES AND TWO ASSUMED TOTAL LUMINOSITIES

M_{LG} ($M_\odot$)	M/L	
	$L_{LG} = 1.1 \times 10^{11}\ L_\odot$	$L_{LG} = 1.5 \times 10^{11}\ L_\odot$
4×10^{11}	3.6	2.7
5×10^{11}	4.5	3.3
2×10^{12}	18	13
5×10^{12}	45	33
2×10^{13}	182	133

© American Astronomical Society • Provided by the NASA Astrophysics Data System

1986ApJ...307....1S

itself, and hence that $\Omega_0 \sim 0.1$ obtained from a variety of arguments (see Sandage and Tammann 1983, 1986) is the best fit to all the known data.

IX. SUMMARY

The principal results of this investigation are the following:

1. A deceleration of the very local cosmological expansion field may be present in the available data for galaxies and groups of galaxies with distances less than 10 Mpc.

2. The effect is small, near the limit of detection, meaning that the velocity field is very nearly linear, even locally (i.e., within ~ 2 Mpc).

3. The mass of the Local Group is less than $5 \times 10^{12}\ M_\odot$ from the available data and the deceleration method. The best fit to the data gives $M_{LG} = 4 \times 10^{11}\ M_\odot$, giving a mass-to-light ratio of ~ 3. The ratio could be as large as ~ 25 if $M_{LG} = 3 \times 10^{12}\ M_\odot$ as an upper limit from the available data. Massive halos with $M/L \gtrsim 100$ for either the Galaxy or for M31 are excluded by the data.

4. The mean random motion about the calculated decelerated velocity-distance relation is $\sigma(v) \approx 60$ km s^{-1}. The true random velocities must be less than this due to uncertainties in the adopted distances. The Local Group mass using this dispersion as a virial velocity is also low and of the order $\sim 4 \times 10^{11}\ M_\odot$.

5. The variation of the Hubble v/r ratio with distance is very small beyond 2 Mpc (Fig. 4) for any reasonable mass of the Local Group. This means that the decelerating effect of the Local Group cannot be invoked to explain any supposed large variation of H with distance locally.

I am grateful for a discussion with Jeremiah Ostriker on the difference in the dynamics of massless satellite particles moving relative to a stationary center of mass and of two massive particles that define the center of mass.

It is also a pleasure to thank Maria Anderson for the difficult preparation of the many drafts of this paper for publication.

REFERENCES

Aaronson, M., Schommer, R. A., and Olszewski, E. W. 1984, *Ap. J.*, **276**, 221.
Arp, H. C., and Sandage, A. 1985, *A.J.*, **90**, 1163.
Baade, W., and Swope, H. H. 1963, *A.J.*, **68**, 435.
Babcock, H. W. 1939, *Lick Obs. Pub.*, No. 498.
Bahcall, J. N., and Tremaine, S. 1981, *Ap. J.*, **244**, 805.
Burbidge, G. 1975, *Ap. J. (Letters)*, **196**, L7.
Demers, S., Kunkel, W. E., and Irwin, M. J. 1985, *A.J.*, **90**, 1967.
de Vaucouleurs, G. 1958, *A.J.*, **63**, 253.
———. 1964, *A.J.*, **69**, 737.
———. 1972, in *IAU Symposium 44, External Galaxies and Quasi-Stellar Objects*, ed. D. S. Evans, D. Wills, and B. J. Wills (Dordrecht: Reidel), p. 353.
———. 1975, in *Galaxies and the Universe*, Vol. **9**, ed. A. Sandage, M. Sandage, and J. Kristian (Chicago: University of Chicago Press), p. 557.
Einasto, J., Kaasik, A., and Saar, E. 1974, *Nature*, **250**, 309.
Einasto, J., and Lynden-Bell, D. 1982, *M.N.R.A.S.*, **199**, 67.
Epstein, E. E. 1964, *A.J.*, **69**, 490.
Freedman, W. L. 1985, in *IAU Colloquium 82, Cepheids: Theory and Observations*, ed. B. F. Madore (Cambridge University Press), p. 225.
Giraud, E. 1986*a*, *Astr. Ap. Letters*, in press.
———. 1986*b*, *Astr. Ap.*, in press.
———. 1986*c*, *Astr. Ap.*, submitted.
Gottesman, S. T., and Hunter, J. H. 1982, *Ap. J.*, **260**, 65.
Graham, J. 1984, *A.J.*, **89**, 1332.
Haggerty, M. J., and Wertz, J. R. 1971, *M.N.R.A.S.*, **155**, 495.
Hartwick, F. D. A., and Sargent, W. L. W. 1978, *Ap. J.*, **221**, 512.
Hawkins, M. R. S. 1983, *Nature*, **303**, 406.
Hubble, E. 1936, *Ap. J.*, **84**, 270.
Humason, M. L., Mayall, N. U., and Sandage, A. 1956, *A.J.*, **61**, 97.
Humason, M. L., and Wahlquist, H. D. 1955, *A.J.*, **60**, 254.
Innanen, K. A., Harris, W. E., and Webbink, R. E. 1983, *A.J.*, **88**, 338.
Kahn, F. D., and Woltjer, L. 1959, *Ap. J.*, **130**, 705.
Kayser, S. E. 1967, *A.J.*, **72**, 134.
Kraan-Korteweg, R. 1985, *Astr. Ap.*, in press.
Lauberts, A. 1976, *Astr. Ap.*, **52**, 309.
Lin, D. N. C., and Lynden-Bell, D. 1977, *M.N.R.A.S.*, **181**, 59.
Lynden-Bell, D. 1981, *Observatory*, **101**, 111.
———. 1982, in *Astrophysical Cosmology: Proceedings of the Study Week on Cosmology and Fundamental Physics*, Vol. **48**, ed. H. A. Brück, G. V. Coyne, and M. S. Longair (Rome: Specola Vaticana), p. 85.
———. 1983, in *Kinematics, Dynamics, and Structure of the Milky Way*, ed. W. L. H. Shuter (Dordrecht: Reidel), p. 349.
Lynden-Bell, D., Cannon, R. D., and Godwin, P. J. 1983, *M.N.R.A.S.*, **204**, 87P.
Lynden-Bell, D., and Lin, D. N. C. 1977, *M.N.R.A.S.*, **181**, 37.
Madore, B. F., and Arp, H. C. 1979, *Ap. J. (Letters)*, **227**, L103.
Materne, J., and Tammann, G. A. 1976, in *Stars and Galaxies from Observational Points of View*, ed. E. K. Kharadze (Tiflis: Abastumani Astrophysical Observatory), p. 455.
Mayall, N. U. 1946, *Ap. J.*, **104**, 290.
McCrea, W. H. 1953, *Rept. Progr. Phys.*, **16**, 321.
McVittie, G. C. 1965, *General Relativity and Cosmology* (Urbana: University of Illinois Press), p. 142.
Miyamoto, M., Satoh, C., and Ohaski, M. 1980, *Astr. Ap.*, **90**, 215.
Ostriker, J. P., and Caldwell, J. A. R. 1983, in *Kinematics, Dynamics, and Structure of the Milky Way*, ed. W. L. H. Shuter (Dordrecht: Reidel), p. 249.
Ostriker, J. P., and Peebles, P. J. E. 1973, *Ap. J.*, **186**, 467.
Ostriker, J. P., Peebles, P. J. E., and Yahil, A. 1974, *Ap. J.*, **193**, L1.
Peebles, P. J. E. 1976, *Ap. J.*, **205**, 318.
Rivolo, A. R., and Yahil, A. 1981, *Ap. J.*, **251**, 477.
Roberts, M. S. 1969, *A.J.*, **74**, 859.
Robertson, H. P. 1933, *Rev. Mod. Phys.*, **5**, 62.
Sandage, A. 1961*a*, *Ap. J.*, **133**, 355.
———. 1961*b*, *Ap. J.*, **134**, 916.
———. 1962, *Ap. J.*, **136**, 319.
———. 1971, *Ap. J.*, **166**, 13.
———. 1975, *Ap. J.*, **202**, 563 (Paper VIII).
———. 1983*a*, *A.J.*, **88**, 1108.
———. 1983*b*, *A.J.*, **88**, 1569.
———. 1984*a*, *A.J.*, **89**, 621.
———. 1984*b*, *A.J.*, **89**, 630.
———. 1986, *A.J.*, **91**, 496.
Sandage, A., and Carlson, G. 1983, *Ap. J. (Letters)*, **267**, L25.
———. 1985*a*, *A.J.*, **90**, 1019.
———. 1985*b*, *A.J.*, **90**, 1464.
Sandage, A., and Hardy, E. 1973, *Ap. J.*, **183**, 743 (Paper VII).
Sandage, A., and Tammann, G. A. 1974, *Ap. J.*, **194**, 223.
———. 1975, *Ap. J.*, **196**, 313 (Paper V).
———. 1982*a*, *Ap. J.*, **256**, 339.
———. 1982*b*, in *Astrophysical Cosmology: Proceedings of the Study Week on Cosmology and Fundamental Physics*, Vol. **48**, ed. H. A. Brück, G. V. Coyne, and M. S. Longair (Rome: Specola Vaticana), p. 23.
———. 1983, *Proceedings of the First ESO/CERN Symposium: Large-Scale Structure of the Universe, Cosmology, and Fundamental Physics*, ed. G. Setti and L. Van Hove (Munich: European Southern Observatory), pp. 127–151.
———, 1985, in *Lecture Notes in Physics*, Vol. **224**, *Supernovae as Distance Indicators*, ed. N. Bartel (Berlin: Springer-Verlag), p. 1.
———. 1986, in *Inner Space/Outer Space*, ed. D. Schramm and M. Turner (Chicago: University of Chicago Press), in press.
Sandage, A., Tammann, G. A., and Hardy, E. 1972, *Ap. J.*, **172**, 253.
Schechter, P. 1980, *A.J.*, **85**, 801.
Silk, J. 1974, *Ap. J.*, **193**, 525.
Suntzeff, N. B., Olszewski, E., and Stetson, P. B. 1985, *A.J.*, **90**, 1481.
Tammann, G. A., and Sandage, A. 1968, *Ap. J.*, **151**, 825.
———. 1985, *Ap. J.*, **294**, 81.
van Albada, G. B. 1962, in *Problems of Extragalactic Research*, ed. G. C. McVittie (New York: Macmillan), p. 411.
Wakamatsu, K.-I. 1981, *Pub. A.S.P.*, **93**, 707.
Wertz, J. R. 1971, *Ap. J.*, **164**, 227.
Yahil, A., Tammann, G. A., and Sandage, A. 1977, *Ap. J.*, **217**, 903.

ALLAN SANDAGE: Mount Wilson and Las Campanas Observatories of the Carnegie Institution of Washington, 813 Santa Barbara Street, Pasadena, CA 91101-1292

© American Astronomical Society • Provided by the NASA Astrophysics Data System